INVESTIGATING THE EFFECT OF STRONTIUM IN BONE MINERAL DENSITY MEASUREMENTS OF TRABECULAR BONE MIMICKING PHANTOMS USING QUANTITATIVE ULTRASOUND

by

Bisma Rizvi

B. Sc., York University

Toronto, Ontario, Canada, 2012

A thesis presented to Ryerson University
in partial fulfillment of the requirements for the degree
of Master of Science in Biomedical Physics

Toronto, Ontario, Canada, 2016

© Bisma Rizvi 2016

AUTHOR'S DECLARATION

I hereby declare that I am the sole author of this thesis. This is a true copy of the thesis, including any required final revisions, as accepted by my examiners.

I authorize Ryerson University to lend this thesis to other institutions or individuals for the purpose of scholarly research.

I further authorize Ryerson University to reproduce this thesis by photocopying or by other means, in total or in part, at the request of other institutions or individuals for the purpose of scholarly research.

I understand that my thesis may be made electronically available to the public.

Bisma Rizvi

ABSTRACT

INVESTIGATING THE EFFECT OF STRONTIUM IN BONE MINERAL DENSITY MEASUREMENTS OF TRABECULAR BONE MIMICKING PHANTOMS USING QUANTITATIVE ULTRASOUND

Bisma Rizvi

Master of Science, Biomedical Physics

Department of Physics, Ryerson University, 2016

Dual-energy x-ray absorptiometry (DXA) is the current gold standard method used for the diagnosis of osteoporosis. However, it is well-established that the presence of strontium in bone could lead to significant error in measurement of bone mineral density (BMD) and diagnosis of osteoporosis using DXA. The objectives of this study are: (1) to develop novel bone-mimicking phantoms containing different concentrations of strontium, and (2) to investigate the effect of bone strontium content on the BMD measurement using quantitative ultrasound (QUS) technique. Measurements using the research and clinical QUS systems showed a strong dependency of the BUA (broadband ultrasound attenuation) of the medium with the BMD. Moreover, increasing strontium concentrations in bone phantoms of up to 3 mol% strontium showed no effect on the BUA or the SOS values measured with either system. Therefore, the QUS technique is independent of level of bone strontium of up to 3 mol/mol [Sr/(Sr+Ca)] %.

ACKNOWLEDEMENTS

I would like to show my appreciation to my supervisors Dr. Ana Pejović-Milić and Dr. Jahan Tavakkoli. They helped me finish my thesis successfully and I could have not done it without them. They contributed their time and effort in mentoring me by preparing me for the future. Dr. Pejović-Milić with her extensive help in my thesis write-up by providing me with specific guidelines that ensured I was completing the required tasks successfully. The completion of my manuscript was because of her dedication in helping me and furthermore gave me opportunities by sending me to a number of conferences, which only she made possible. Dr. Milic and Dr. Tavakkoli have guided me in my thesis and helped me with their time when I encountered problems and helped me learn more about myself than I ever have. Their constant support and positive outlook has made me stronger and have made me realize my potential by treating me like family.

I would like to give my gratitude and appreciation to Eric Da Silva who was constantly guiding me throughout this project and who I could have not finished successfully without. He was constantly helping me with my experiments and my journal manuscript preparation. Additionally, I would like to thank Graham Pearson and Arthur Worthington for helping me constantly with their time and effort throughout my experimentation and their technical expertise, and Pooya Sobhe Bidari who helped me with my experiments. I would like to thank Dr. Michael Kolios' group members who were extremely helpful and helped through my master's thesis, especially Dr. Elizabeth Berndl.

I would also like to thank Dr. Luba Slatkovska and Dr. Angela M. Cheung, both from University Health Network, Osteoporosis Program, for their constant help and guidance in my

project and for their support and expertise in the clinical QUS measurements performed in their clinical site.

I would like to thank my committee member Dr. Raffi Karshafian for guiding me in my project and always being available to provide feedback to further my knowledge in my research.

I would also like to thank Dr. Carl Kumardas for his support and believing in me as a graduate student and helping me finish successfully. I would also like to thank Adriana Gaertner for her guidance in the end of my research. Lastly, I would like to show my appreciation to my family who supported me through my entire MSc thesis without whom my life would not be complete.

Table of Contents

AUTHOR'S DECLARATION ..... **ii**

ABSTRACT ..... **iii**

ACKNOWLEDEMENTS ..... **iv**

LIST OF SYMBOLS ..... **viii**

LIST OF ABBREVIATIONS ..... **x**

LIST OF FIGURES ..... **xi**

CHAPTER 1: INTRODUCTION **1**

1.1 OSTEOPOROSIS 1

1.2 STRONTIUM AND ITS EFFECT ON BONE 2

1.3 CLINICAL METHODS TO MEASURE BONE MINERAL DENSITY 6

1.3.1 Dual-Energy X-ray Absorptiometry (DXA) 6

1.3.2 Physics of Dual-Energy X-ray Absorptiometry 7

1.4 QUANTITATIVE ULTRASOUND (QUS) 10

1.4.1 Physics Basis of Bone Evaluation using Quantitative Ultrasound 11

1.4.1.1 Acoustic Attenuation 14

1.4.1.2 Quantitative Ultrasound for Bone Mineral Density Measurement 17

1.4.1.3 QUS Attenuation Measurement 19

1.4.1.4 QUS Speed of Sound Measurement 19

1.5 BONE-MIMICKING TISSUE PHANTOMS 20

1.6 THESIS HYPOTHESIS AND SPECIFIC AIMS 21

1.7 REFERENCES FOR CHAPTER 1 22

CHAPTER 2: BONE MINERAL DENSITY MEASUREMENTS OF STRONTIUM-RICH TRABECULAR BONE MIMICKING PHANTOMS USING QUANTITATIVE ULTRASOUND **29**

2.1 INTRODUCTION 32

2.2 MATERIALS AND METHODS 35

2.2.1 Preparation of Trabecular Bone-Mimicking Phantom 35

2.2.2 Multi-Layer Trabecular Bone-Mimicking Phantoms 36

2.2.3 Research Quantitative Ultrasound System....37
2.2.4 Clinical Quantitative Ultrasound System....39
2.2.5 Statistical Treatment of Data....39
2.3 RESULTS....40
2.3.1 Density of the Trabecular Bone-mimicking Phantoms....40
2.3.2 Quantitative Ultrasound Measurement of the Multi-Layer Trabecular Bone-Mimicking Phantoms....41
2.3.3 Quantitative Ultrasound Index (QUI) of the Multi-Layer Trabecular Bone-Mimicking Phantoms....43
2.4 DISCUSSION....44
2.5 CONCLUSIONS....48
2.6 ACKNOWLEDGMENTS....49
2.7 REFERENCES....50
CHAPTER 3:DISCUSSIONS, CONCLUSIONS, AND FUTURE WORK....54
3.1 DISCUSSIONS....54
3.2 CONCLUSIONS....55
3.3 FUTURE WORK....56
3.4 REFERENCES FOR CHAPTER 3....58
Appendix A: Procedure for Developing Trabecular Bone-mimicking Phantoms....59
Appendix B: Figures of Multi-layer Bone-mimicking Phantom and QUS Systems used in this Study....61
Appendix C: Plot of QUI vs. BMD....63
Appendix D: Measurements of BUA and SOS....64
References for Appendices....65

LIST OF SYMBOLS

x	Thickness (m)
I	Ultrasound intensity through the tissue (W/m^2)
I_o	Incident ultrasound intensity (W/m^2)
μ	Absorbing coefficient of the material (cm^{-1})
μ_l	Linear attenuation coefficient (cm^{-1})
μ_m	Mass attenuation coefficient ($cm^2.g^{-1}$)
μ_T	X-ray linear attenuation coefficient of tissue (cm^{-1})
μ_W	X-ray linear attenuation coefficient of water (cm^{-1})
ρ	Density (g/cm^3)
ρ_e	Effective mass density (g/cm^{-3})
c	Speed of sound (m/s)
M_e	Effective elastic modulus
Z	Acoustic impedance (MRayl)
i, t, r	Indexes for incident, transmitted and reflected beams
Z_1	Impedance of incident wave (MRayl)
Z_2	Impedance of transmitted wave (MRayl)
λ	Wavelength (m)
α	Ultrasound amplitude attenuation coefficient (dB/cm)
α_o	Ultrasound attenuation coefficient at f_c (attenuation intercept) (dB/cm)
α_s	Ultrasound amplitude scattering coefficient (cm^{-1})
α_a	Ultrasound amplitude absorption coefficient (cm^{-1})
β	Ultrasound least squares attenuation slope (attenuation slope) (dB/(cm.MHz))
β_1	Ultrasound attenuation factor ($dB/(MHz^y.cm)$)
β_0	Ultrasound attenuation intercept in the power law model (dB/cm)
f	Frequency (Hz)
A	Atomic number

$d\bar{I}$	Time average ultrasound intensity (W/m^2)
$d\bar{I}_s$	Time average ultrasound scattering intensity (W/m^2)
$d\bar{I}_a$	Time average ultrasound absorption intensity (W/m^2)
P	Acoustic pressure (Pa)
P0	Acoustic pressure amplitude at the source (Pa)
v	Particle velocity of the material (m/s)
E	Young's modulus
θ_1, θ_2	Incident and refractive angle (°)

LIST OF ABBREVIATIONS

BMC	Bone mineral content
BMD	Bone mineral density
BUA	Broadband ultrasound attenuation
DPA	Dual Photon Absorptiometry
DXA	Dual-energy x-ray absorptiometry
QCT	Quantitative computed tomography
QUI	Quantitative ultrasound index
QUS	Quantitative ultrasound
SOS	Speed of sound
TT	Transverse transmission

LIST OF FIGURES

FIG. 1-1: Reflection and refraction at the boundary [36]. 13

FIG. 1-2: Attenuation, absorption and scattering (a) incident wave on a specimen and its scattered, absorbed and attenuated waves (b) Intensity absorbed by an incremental distance dx [33]. 14

FIG. 1-3: Summary of published experimental results for attenuation versus frequency and the power-law dependence on frequency [33]. 16

FIG. 1-4: Transverse transmission setup for BMD measurement using (a) placement of transducers in the mediolateral direction, (b) and (c) Determing SOS thorugh the signal of the reference and then the object (e) BUA calculation by obtaining the slope of the frequency spectra [34]. 18

FIG. 1: The relationship between the total phantom mass density (ρ) and BMD of the trabecular bone-mimicking phantoms prepared for this study. 40

FIG. 2: Relationship between BUA and BMD, and, SOS and BMD, without any strontium present in trabecular bone-mimicking and multi-layer phantoms, as measured with the research and clinical QUS systems. .....……41

FIG. 3: The BUA and SOS as a function of strontium concentration, at a BMD of 200mg/cm^3. 42

FIG. 4: The QUI as a function of strontium concentration in the multi-layer trabecular bone mimicking phantoms using the research and clinical QUS systems.....43

FIG. 5: Bland-Alman plot of the QUI determinations. Mean difference of 5.9 and standard deviation (*s*) of 0.5 .....…… 44

FIG. A-1: Bone-mimicking phantom moulded containing HA and gelatine.....……59

FIG. B-1. Schematic design of the multi-layer bone-mimicking phantom using castor oil to mimic soft tissue. 61

FIG. B-2. Schematic experimental setup of research QUS system for determination of BUA and SOS. 61

FIG. B-3: Schematic experimental setup of clinical QUS (Hologic Sahara® QUS system) with acrylic container for the determination of BUA and SOS. 62

FIG. C-1: The QUI as a function of BMD concentration in the multi-layer trabecular bone-mimicking phantoms using the research and clinical QUS systems.....63

CHAPTER 1:INTRODUCTION

1.1 OSTEOPOROSIS

Osteoporosis is a bone disease characterized by reduced bone mass and micro architectural deterioration of bone tissue causing susceptibility to fracture [4]. Osteoporosis might linger undiagnosed for years until the occurrence of fractures; spine, hip and wrist joints as the most frequent sites of fracture. This may lead to long-term physiological, social and financial distress resulting in mortality, long-term morbidity and considerable health care cost. Over 1.3 million fractures occur annually in the US in adults aged 45 and above, of which, 70% are a direct or indirect consequences of osteoporosis [5]. Hence, early diagnosis is a key factor in prevention of these fractures.

The current gold standard for diagnosis of osteoporosis is dual energy X-ray absorptiometry (DXA) which measures bone mineral density (BMD), reflecting the strength of bones as represented by content of calcium [4]. The diagnostic criteria for this widely validated technique, is derived from the T-score and Z-scores obtained from the BMD of the subject. The T-score is determined by comparing the patients measured BMD with that of expected in a normal, healthy adult of the same gender and the Z-score value takes into account patients age as well as gender (considers decreases in BMD values as a consequence of aging) [6]. Initially, the T-score is arbitrarily assigned an average value of 50 [6]. For each standard deviation (SD) from the average, the T-score increases or decreases by 10 points therefore one SD from the average would be 60. In contrast, Z-score uses a scale that assigns 0 as the initial average value and one SD in this scale is an increase or decrease by 1 [7].

According to the WHO, osteoporosis is defined as having a BMD value that lies within two and a half negative standard deviations (SD) of the mean BMD value of healthy adults (T-score < -2.5SD). Osteopenia (a precursor to osteoporosis) is described as having a BMD value between two and a half to one standard deviation below the mean (T-score = -2.5 to -1.0SD). BMD values above one negative standard deviation or more are classified as normal (T-score ≥ -1.0 SD) [8].

Even though osteoporosis is currently incurable, several treatments are currently available that may help to decrease the rate of bone deterioration. Treatments to influence bone remodelling may facilitate bone turnover in osteoporotic patients. Bone remodelling consists of bone formation and it is opposite to bone resorption (depletion). It is imperative that there be an adequate remodelling balance between the bone forming osteoblasts and their counter parts the osteoclasts [9]. When this balance is disturbed, it results in osteoporosis. In osteoporotic patients the bone decomposition is much faster than bone formation and hence the treatments of osteoporosis include targeting either one. The proposed classification of drugs used to treat osteoporosis consists of anti-catabolic (inhibiting osteoclast formation or resorption), anabolic (stimulating bone formation) and combination therapy. These may result in an increase in strength, geometry, material properties such as BMD and microstructure of the bone [10].

1.2 STRONTIUM AND ITS EFFECT ON BONE

Strontium (Sr: Molecular weight =87.62, and Atomic number =38) is an alkaline earth metal of Group II, positioned directly under Calcium in the periodic table. Low concentrations of it ranging from 0.021 up to 0.37 mg/l are present in natural water sources such as rivers, springs and wells. Nutritional sources such as meat, poultry, vegetables and fruit contain concentrations

ranging from 0.3 to 5.1 mg/kg. Higher concentrations occur in cereals, grains and seafood up to 25 mg/kg. Hence, dietary intake and geographical location have a substantial impact on the levels of strontium, which vary greatly in adults [11].

We will study the benefits of low doses of strontium, however it should be noted that toxic effects have been regularly observed, in humans due to exposure to high concentrations of strontium; and toxicity, due to administration of high levels of strontium on animals has also been extensively studied [11].

Radioactive strontium isotopes are used widely for medical therapeutic and diagnostic purposes. The therapeutic use of strontium was recognized with strontium-89 to treat ostealgia (bone pain) resulting from metastatic prostate cancer. Also, strontium-85 and 88 are bone markers in diagnosis as a marker for calcium metabolism [11].

Strontium is distributed throughout the body and is mainly deposited in the bone and the teeth causing either detrimental or beneficial effects depending on the concentration of the administered dose [10].

Strontium ranelate, a medication that is used as a treatment for osteoporosis, is an orally administered anti-osteoporotic drug that has been shown to prevent bone loss and an increase in bone strength experimentally [12]. This medication, when given to patients, enhances bone cell replication and formation.

Strontium is incorporated into the bone heterogeneously and is prominent in newly formed bone by two methods: surface exchange and ionic substitution. Ionic substitution is a process of replacing calcium ions by other ions in the crystal during formation. Surface ionic exchange occurs at the surface of the crystal through rapid exchange between blood and the surface of bone [10].

The strontium and calcium ions differ considerably in size due to the difference in ionic radius. This causes the crystal to change shape, size and structure [13].

In vitro and *in vivo* studies have shown that strontium enhances the replication of pre-osteoblastic cells (cells which stimulates bone formation while decreasing bone resorption) [14]. Treatment with low doses of strontium, will show an increase in osteoid and osteoblast surfaces further leading to a rise in the number of bone-forming sites without the detrimental side effect of excessive bone mineralization. Strontium has been known to play an anabolic and anti-catabolic role in bone metabolism [15]. Pre-clinical studies have revealed the beneficial effects of strontium ranelate on bone metabolism.

A study performed to modulate long term efficacy for strontium ranelate on vertebral bone metabolism in adult mice demonstrated an increase in bone formation and a decrease in bone resorption, resulting in an increase in vertebral bone mass [16]. This was also observed in the mandibular bones of, otherwise normal, adult monkeys [17]. Other studies have shown that strontium ranelate can cause an increase in bone strength in normal or osteopenic animals. Two independent studies concluded that the treatment with strontium ranelate promoted facture healing by the enhancement of bone and tissue volume (within the callus), and results in formation of a more mature and tightly arranged bone (8 week study on overiectomized rats (ovyx) where ovaries of female rats have been removed. [15, 16]. Also, Marie *et al* (1993) treated ovyx osteopenic rats with a strontium salt for 60 days, which resulted in the improvement of bone mineral content and an increase in trabecular bone volume while maintaining bone mineral density [20]. This process was observed using histologic examination of bone samples where an increase in osteoid surface resulted from a rise in osteoblastic activity. Furthermore, beneficial effects were seen at low doses of strontium compared to calcium when given to rats with normal renal function, where calcium

supplements fail to recalcify osteopenic areas; most likely due to strict homeostatic control of calcium levels [10].

Clinical studies have been performed to determine the beneficial effects of strontium on bone. A clinical study on placebo–controlled trail (PREVOS) displayed the ability of strontium to prevent bone loss due to oestrogen deficiency [21]. Early postmenopausal women were given either strontium (1g/day) for duration of two years or a placebo. This resulted in significant improvements in BMD measured by DXA, compared to those in the placebo group in the lumbar spine (2.4%), femoral neck (3.3%) and total hip (4.1%). The SOTI (*Spinal Osteoporosis Therapeutic Intervention)*, a randomized, double-blinded and placebo-controlled clinical trial was based on 1649 of postmenopausal women with osteoporosis. They were either given (2g/day) of strontium ranelate or placebo. It was noted a 41% reduction in the risk of new vertebral fracture over 3 years compared to the placebo [22]. In another, study called TROPOS (treatment of peripheral osteoporosis), a randomized, double-blinded, placebo-controlled clinical trial, where strontium was given to 5091 postmenopausal women. This group showed a significant decrease in the risk of new non-vertebral fractures by 33% and an increase of 6.5% in femoral neck BMD. SOTI and TROPOS were studied extensively and revealed a bone turnover with an increase in bone formation and a decrease in bone resorption.

However, in spite of the above-mentioned benefits of strontium, at higher doses, negative effects have been documented, such as undesirable changes due to bone mineralization leading to a decrease in BMD [10]. Since too much or too little mineral can cause a negative impact on bone health. Ionic exchange between strontium and calcium causes significant decrease in the calcium content, which leads to distortion of the crystal lattice. This alteration in the crystal may weaken the growth of the crystal, as it inhibits mineralization because difference in size of the element

decreases the strength of the chemical bonds [23]. Oste et al. were the first to demonstrate the deleterious effects of high doses of strontium on bone (3g/l). It was reported that higher doses may induce osteomalacia in chronic renal failure rats by causing an excessive increase in osteoid surfaces and a reduction in bone mineralization [24]. Other studies have shown adverse effects of high concentrations of strontium on bone due to a decrease in formation and an increase in resorption [25].

Dual energy X-ray absorptiometry (DXA) is the current method of choice used for monitoring of osteoporosis therapy and diagnosis of the disease itself. It is a non-invasive technique that measures areal bone mineral density (areal BMD or aBMD), bone mineral content divided by bone area in square centimeters, primarily of the hip and lumbar spine regions. DXA measurements are based on the attenuation of X-rays through bone. Since presence of strontium leads to higher X-ray attenuation in comparison to calcium in bone, its presence in the body leads to an overestimation of aBMD in DXA measurements. This can be a major downside of DXA, when monitoring osteoporosis therapy supplemented with strontium at low dosages [26].

1.3 CLINICAL METHODS TO MEASURE BONE MINERAL DENSITY

1.3.1 Dual-Energy X-ray Absorptiometry (DXA)

The first validated technique of the BMD measurement was single photon absorptiometry (SPA) of the forearm [7]. However, its applicability was only to the peripheral skeletal sites, and therefore Dual Photon Absorptiometry (DPA) was developed for BMD measurements of the axial body [27]. Later advances led to the replacement of these by Dual-Energy X-ray Absorptiometry, commonly referred to as DXA. DXA has become the gold standard since 1980s for bone densitometry, due to its image precision, scan speed and low radiation exposure. It is capable of

distinguishing between several regional components such as bone mineral and (fat or lean) soft tissue [28]. The fundamental principle behind DXA measurement is the utilization of the "through transmission" technique, which requires two photon X-ray energies. These two different energies are necessary to distinguish between bone and soft tissue. X-ray production occurs by ejecting and accelerating electrons at the cathode and then traveling to the higher voltage metal target (anode). The collision of impinging electrons with the nucleus of the anode's atom causes production of other X-rays (bremsstrahlung radiation). When the impinging electrons are given sufficient energy to knock out an electron in the anode's atom from its shell, then a higher shell electron can fill the vacant energy state. The emitted radiations from this process are called characteristic X-rays. These emit a specific energy that corresponds to each energy state (electron shell) [29].

1.3.2 Physics of Dual-Energy X-ray Absorptiometry

DXA is a diagnostic modality that uses two narrow beams of mono-energetic photons to determine bone mineral density (BMD) of bone in presence of soft tissue. The majority of the attenuation in bone and soft tissue happens by Compton scattering and photoelectric absorption. Photoelectric effect occurs when a photon interacts with an inner shell electron and an electron is ejected. Compton scattering is the interaction of an incident photon with an outer shell electron (loosely bound), resulting in an ejected electron and a scattered photon with smaller energy than the incident photon [24, 25]. The attenuation caused by a mono-energetic narrow beam of X-ray radiation passing through a homogeneous material (tissue) can be explained using the following:

$$I = I_0 \exp(-\mu_l \cdot x) \tag{1-1}$$

where I_0 is the incident intensity, I is the intensity of X-rays after passing through x, the thickness of tissue and μ_l is the linear attenuation coefficient of the tissue (cm^{-1}). μ_l is the fraction of the X-ray beam that is absorbed per unit thickness of the absorber. The attenuation coefficient is

dependent on the photon energy, tissue composition and the physical density (ρ) represented here in g/cm^3 [7].

The linear attenuation coefficient is replaced by mass attenuation coefficient μ_m(cm$^{2/}$g) where $\mu_l/\rho = \mu_m$ in equation 1-2.

$$I = I_0 \exp(-\mu_m \rho x) \tag{1-2}$$

A mono-energetic beam that travels through bone, surrounded by soft tissue is represented by equation 1-3, where "*B*" and "*S*" are superscripts that denote bone and soft tissue respectively.

$$\left(\frac{I}{I_0}\right) = \exp(-(\mu_m^S(\rho x)^S + \mu_m^B(\rho x)^B)) \tag{1-3}$$

To determine the mass attenuation coefficients of bone and soft tissue, two different photon energies are utilized. Hence, two x-ray attenuation equations are generated, (equations 1-4 and 1-5) where $(\rho x)^B$ and $(\rho x)^S$are the aBMD of bone and soft tissue respectively [7].

$$\left(\frac{I}{I_0}\right)_L = \exp(-(\mu_{m,L}^S(\rho x)^S + \mu_{m,L}^B(\rho x)^B)) \tag{1-4}$$

$$\left(\frac{I}{I_0}\right)_H = \exp\left(-\left(\mu_{m,H}^S(\rho x)^S + \mu_{m,H}^B(\rho x)^B\right)\right) \tag{1-5}$$

Rearranging equations 4 and 5 gives the following equations for aBMD;

$$(\rho x)^B = \frac{\log\left(\frac{I}{I_0}\right)_H - \left(\frac{\mu_{m,H}^S}{\mu_{m,L}^S}\right)\cdot\log\left(\frac{I}{I_0}\right)_L}{\mu_{m,H}^B - \left(\frac{\mu_{m,H}^S}{\mu_{m,L}^S}\right)\cdot\mu_{m,L}^B} \tag{1-6}$$

$$(\rho x)^S = \frac{-\log\left(\frac{I}{I_0}\right)_H + \left(\frac{\mu_{m,H}^B}{\mu_{m,L}^B}\right)\cdot\log\left(\frac{I}{I_0}\right)_L}{-\mu_{m,H}^S + \left(\frac{\mu_{m,H}^B}{\mu_{m,L}^B}\right)\cdot\mu_{m,L}^S} \tag{1-6}$$

The ratio used above, $\frac{\mu_{m,H}^S}{\mu_{m,L}^S}$, is called the R-value and is measured at a location where bone is not present in the scan path $\mu_B = 0$. Where, $\mu_{m,H}^S$ and $\mu_{m,L}^S$ denote the mass attenuation coefficients of soft tissue determined by high and low energies respectively [7].

$$R_S = \frac{\mu_{m,H}^{s}}{\mu_{m,L}^{s}} = \left| \frac{\ln\left(\frac{I}{I_0}\right)_L}{\ln\left(\frac{I}{I_0}\right)_H} \right|_{\mu_B=0} \tag{1-7}$$

Since the modality does not take into account the true volumetric bone density but rather the aBMD only (g/cm^2), the accuracy of DXA measurements is affected by the projected area. Since the BMD determined by DXA is two-dimensional, therefore the thickness of the bone can have an effect on the value of BMD (overestimating BMD for thicker bones) [31]. Also, its precision can be adversely affected by increase in age, increase in weight (for the femur bone) and by a reduction in density values [32]. The current DXA systems have a precision error of 1.0% for the entire body, ~0.5-1% for the spine, 2.0-5.0% for the femoral neck (depends on the anatomic size) [33]–[35].

The assumption made by DXA is known as the "two-component limitation" where DXA can only accurately analyse two components of bone and soft tissue. However, there are four-components in the body that need to be considered, i.e. bone mineral, fat-free soft tissue, fat and water [7]. DXA has the ability to distinguish lean tissue from fat tissue in areas where there is no bone. It determines the attenuation values of soft tissue closest to the bone and makes an assumption about the composition of fat distribution to distinguish between lean and soft tissue around the bone. The presence of metal artefacts (jewellery, implants etc.) for subjects undergoing DXA scans may cause a deterioration of accuracy in measurement that is inestimable. Prior to DXA scanning, subjects are required to remove jewellery where permanent implants (surgical, dental etc.) may be a cumbersome impediment to accurate diagnoses.

In bone density measurements, internal machine errors that are different for each manufacturer must be taken into consideration when dealing with a patient [36]. The variations in each system include: dual-energy production, calibration procedures, edge detection algorithms

and assumptions regarding fat distribution. Each of these in turn depends on the thickness of the patient and the motion and stability of a patient during measurement.

1.4 QUANTITATIVE ULTRASOUND (QUS)

In quantitative ultrasound (QUS) the assessment of bone density is measured on the basis of several parameters, unlike DXA which uses only the aBMD to determine the quality of bone. Hence, QUS may provide additional information about the structural and material properties but is still being extensively researched [37].

Ultrasound waves are high frequency sound waves outside the human hearing range. These mechanical waves can be represented by sinusoidal waves. They transport energy through a medium by causing longitudinal displacement of the particles inside the medium [2].

In non-viscous fluids, the ultrasound waves travel longitudinally along the direction of propagation without generating shear waves. Conversely, in viscous fluids and solids, strong bonds between particles induce a shearing strain that can be transmitted to adjacent layers in the form of transverse waves [3].

In hard tissues such as bones both longitudinal and shear waves must be taken into consideration as their heterogeneous structures cause the waves to behave very differently in the two components: the trabecular bone (spongy inside layer) and surrounding cortical bone (dense layer). The oscillation of the particles inside the medium causes rarefaction and compression as ultrasound waves propagate. Positive pressure is a result of the compression and negative pressure is a result of the rarefaction of the particles. The SI unit for measuring pressure is Pascal where 1 Pa=1 N/m^2. The amount of pressure is directly proportional to the magnitude of displacement of the particle from its initial position i.e. amplitude of the ultrasound signal [38].

1.4.1 Physics Basis of Bone Evaluation using Quantitative Ultrasound

As ultrasound waves propagate in a medium, they transport energy. The power of the ultrasound wave, i.e. energy transferred per unit of time, that is flowing through a unit area is known as its intensity, I, with units of W/m^2 [38].

The propagation of a monochromatic ultrasound wave in time and space can be represented in terms of its frequency f, period T and wavelength λ:

$$\lambda = \frac{c}{f} = cT \tag{1-8}$$

where the wave propagation velocity (or speed of ultrasound) is c. The frequencies that are generally used in diagnostic ultrasound in today's clinical applications are typically in the range 2-25 MHz.

Acoustic impedance Z is the measure of the response of the particles in the medium (similar to resistance in electrical current and refractive index in optics), to a wave of given pressure with units of $kg.m^{-2}s^{-1}$. The term Rayl is often used to express this unit [38]. During the propagation of an ultrasound wave the medium's particles will vibrate and cause displacement parallel to their resting positions. The velocity of this displacement is called acoustic particle velocity v. Hence, the particle velocity being the speed of motion of the particles that are caused by the ultrasound wave and is different from ultrasound velocities. In a non-attenuating medium plane waves are related to particle velocity (v) and sound pressure (p) by:

$$p = \rho c v = Zv \tag{1-9}$$

therefore,

$$Z = \rho c \tag{1-10}$$

where ρ is the medium's density.

The speed of propagating ultrasound waves depends on the density and the stiffness which is a measure of compressibility of the medium. However, to account for the wave type such as; bulk compression, bulk shear, and surface or guided-wave-specific differences, the effective elastic modulus M_e and effective mass density ρ_e (equation 1-12) are used to generalize the differences in c for each wave type. The M_e value determines the effective stiffness and ρ_e the effective density for each wave type: [7].

$$c = \sqrt{\frac{M_e}{\rho_e}} \tag{1-11}$$

In trabecular bone, the Young's modulus (E) for a longitudinal wave, represents strength of elasticity. The direct relationship of propagation velocity to stiffness (Young's modulus) may be used for the assessment of bone strength (equation 1-13).

$$c = \sqrt{\frac{E}{\rho}} \tag{1-12}$$

The reflection of ultrasound wave is determined by the difference in acoustic impedance of the two media. When the acoustic impedance of a material is different from the surrounding then some of incident waves (i) are transmitted (t) and some are reflected (r). The ratio of reflected to incident intensities can be determined by the reflection coefficient as

$$\frac{I_r}{I_i} = R_i = \left(\frac{Z_1 - Z_2}{Z_1 + Z_2}\right)^2 \tag{1-13}$$

Reflection occurs when the ultrasound wave encounters an interface that is much larger compared to the wavelength of the wave. When this wave encounters an interface that is comparable to or smaller than the wavelength then the laws of reflection are ignored and scattering takes place [2]. If the wavelength λ, is much smaller than the size of the target d, the wave is scattered uniformly ($\lambda \ll d$). The total scattered power for a small object is lower than for a large object and is related to the size and wavelength by

$$W_s \propto \frac{d^6}{\lambda^4} \propto d^6 f^4 \tag{1-14}$$

since $1/\lambda$ is proportional to f. The frequency dependence for a small target is referred to as Rayleigh scattering [38].

If a plane wave impacts a smooth interface, a reflected and transmitted wave will be generated (figure 1-1). The reflected and transmitted have coefficients, which determine the energy reflected and transferred through the material. The amount of energy transferred to a material is dependent on the acoustic impedance of the two interfaces or boundaries.

Mathematically,

$$T = 1 - R = T = \frac{4Z_1Z_2}{(Z_1+Z_2)^2}. \tag{1-15}$$

where Z_1 and Z_2 are characteristic acoustic impedance of the first and second media for longitudinal waves respectively. T is the transmission coefficient and R is the reflection coefficient.

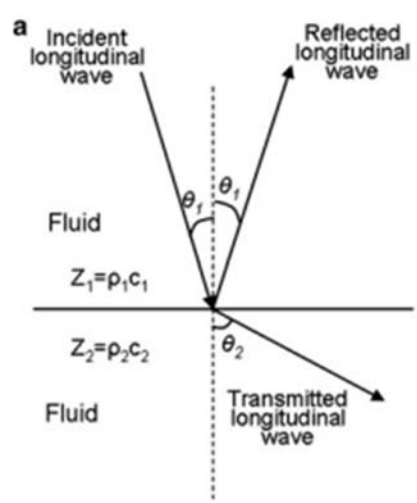

FIG. 1-1: Reflection and refraction at the boundary [1].

The speed of the longitudinal waves is much larger than that of the shear waves. The existence of the shear waves is neglected in most practical applications. As for QUS assessment of bones, a number of research work has been conducted in using shear ultrasound waves using

the USR technique. Recently a clinical device has been introduced for QUS bone assessment with measurement based on the arrival of the wave with the fastest speed (longitudinal or shear) called the Sunlight Omnisense™ (Sunlight Ultrasound Technologies Ltd., Rehovot, Israel) [4, 26, 33, 34].

1.4.1.1 Acoustic Attenuation

Acoustic attenuation is the decrease in intensity of the ultrasound wave with distance travelled [3]. This decrease in intensity can be represented by the exponential function, which shows that for each centimetre of propagation, a constant fractional decrease in intensity occurs (figure 1-2).

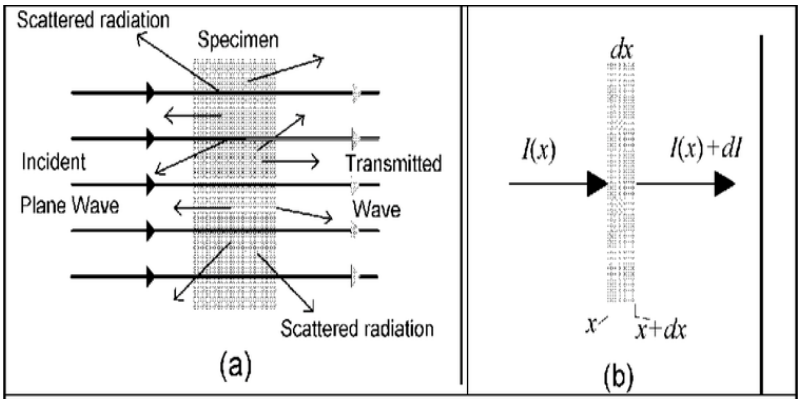

FIG. 1-2: Attenuation, absorption and scattering (a) incident wave on a material and its scattered, absorbed and attenuated waves (b) Intensity absorbed by an incremental distance *dx* [2].

The two different mechanisms that contribute to ultrasound attenuation are absorption and scattering. Absorption is a process where ultrasound energy is converted into other forms of energy such as heat, chemical energy, light, etc. The ultrasound wave may also be attenuated by re-direction of some of the energy (by scattering).

Absorption of ultrasound is dependent on the composition and structure of the medium. Since the adjacent medium's particles are moving with varying velocities, this leads to absorption due to

friction. Acoustic attenuation of the trabecular bone is greater than the cortical bone due to its porous structure and viscosity [3].

Scattered and absorbed power over an incremental distance *dx*, will be proportional to the time-averaged intensity $\bar{I}$ and contribute to the loss of the transmitted beam intensity of:

$$d\bar{I}_s = -2\alpha_s\bar{I}(x)dx, \ and \ \ d\bar{I}_a = -2\alpha_a\bar{I}(x)dx \tag{1-16}$$

where α_s and α_a are the scattered and absorption coefficients respectively. Combining these two processes the intensity becomes:

$$d\bar{I} = d\bar{I}_s + d\bar{I}_a = -2(\alpha_s + \alpha_a)\bar{I}(x)dx \ \ or \ \frac{d\bar{I}}{\bar{I}(x)} = -2(\alpha_s + \alpha_a)dx \tag{1-17}$$

by integrating the intensity at location x can be determined, where $\bar{I}(0)$ is the intensity at x=0:

$$\bar{I}(x) = \bar{I}(0)e^{-2(\alpha_s+\alpha_a)x} = \bar{I}(0)e^{-2\alpha x} \tag{1-18}$$

where α is the sum of scattering and absorption coefficients $(\alpha_s + \alpha_a)$ called amplitude attenuation coefficient.

By taking the log of base 10 of both sides in equation 21 and multiplying by 10 we obtain:

$$10log\left(\frac{\bar{I}(0)}{\bar{I}(x)}\right) = 20\alpha_{NP}xlog(e) = 8.686\alpha_{NP}x. \tag{1-19}$$

By defining α_{dB}=8.686α_{NP} the attenuation coefficient can be represented in terms of pressure and is expressed in dB/cm (decibels per cm) as:

$$\alpha_{dB} = \frac{10}{x}log\left[\frac{\bar{I}_o(0)}{\bar{I}_o(x)}\right] \tag{1-20}$$

The rate at which the wave is attenuated with respect to distance is called the attenuation coefficient [2]. Where *x* represents the thickness of the material. In terms of pressure the attenuation coefficient becomes:

$$\alpha_{dB} = \frac{20}{x}log\left[\frac{p_o(0)}{p_o(x)}\right] \tag{1-21}$$

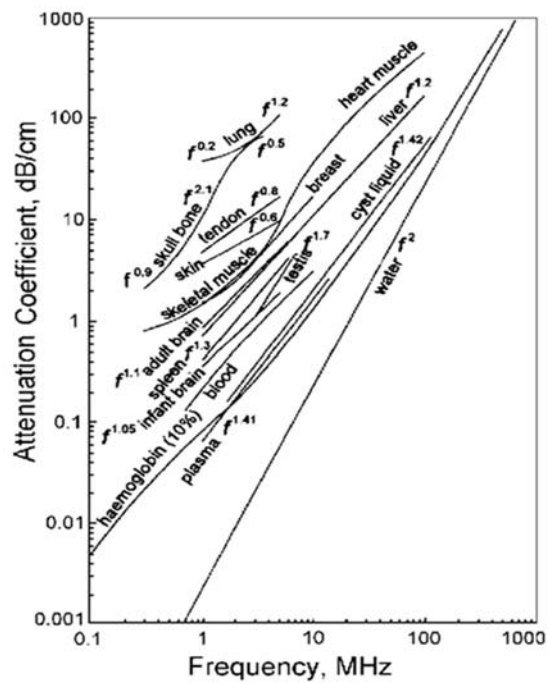

FIG. 1-3: Summary of published experimental results for attenuation versus frequency and the power-law dependence on frequency [2].

Attenuation measurements and its frequency dependence on biological tissues have been extensively studied. Figure 1-3 provides a summary of experimental results from different attenuation measurements under a variety of experimental conditions. The attenuation of bone has a nearly linear dependence on frequency, if the frequency is limited between range of 0.3 to 2 MHz [1]. The attenuation dependence on frequency with good approximation is given by:

$$\alpha(f) = \beta_0 + \beta_1 |f|^y \tag{1-22}$$

where β_0 is the intercept and is usually zero, y is a power law exponent that lies within 1 to 2 and β_1 is the attenuation coefficient in $\frac{dB}{MHz^y \cdot cm}$. The results of previous studies has portrayed a linear dependence of attenuation on frequency for calcaneal bone yields y = 1 and β_1 within a range between 14-20$\frac{dB}{MHz \cdot cm}$ [1].

1.4.1.2 Quantitative Ultrasound for Bone Mineral Density Measurement

There are several clinical QUS devices available that are used to determine the BMD of a patient in calcaneal heel bone [3]. The transverse transmission technique is the most common method used for QUS measurements on devices such as: Achilles (Lunar Co., Madison, WI, USA), UBA 575+ (Hologic Inc., Waltham, MA, USA), and Sahara (Hologic Inc., Waltman, MA, USA). This method has been applied to conduct BMD measurements for patients where DXA is not easily accessible. Transverse transmission technique requires two piezoelectric transducers, consisting of a transmitter and a receiver and it placed on opposite sides of the skeletal site to be measured. The measurements are performed at the most favourable site that consists of 90% trabecular bone. For signal analysis the substitution method is used where the signal transmitted through the bone of interest is compared with the signal transmitted through a reference medium such as water with known values for broadband ultrasound attenuation (BUA) and speed of sound SOS (figure 1-4).

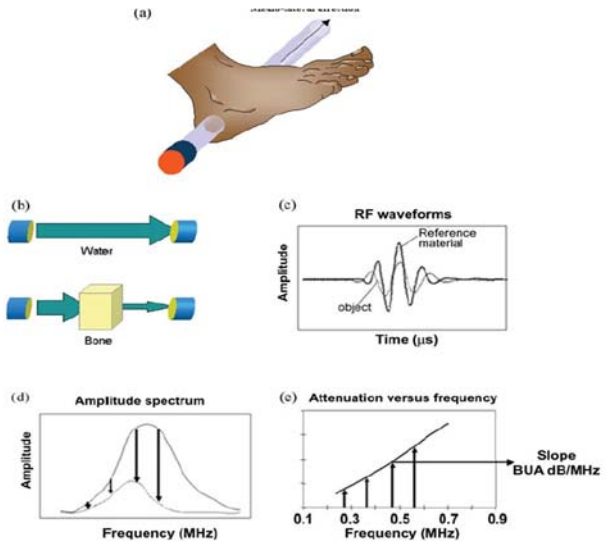

FIG. 1-4: Transverse transmission setup for BMD measurement using (a) placement of transducers in the mediolateral direction, (b) and (c) Determining SOS through the signal of the reference and then the object, and (e) BUA calculation by obtaining the slope of the frequency spectra. [3].

Calcaneal (heel) bone was the first site for which *in vivo* QUS measurements were performed. Human bones are regenerating continuously, usually on the surface of the trabecular tissue, and the changes due to osteoporosis are frequently observed in areas that consist predominantly of trabecular bone (e.g. calcaneal) [3]. This has been widely used *in vitro* using transverse transmission and pulse-echo (PE) configurations [39].

Ultrasound interactions with bone are due to reflection, refraction, scattering and absorption. There has been success in the determination of SOS and BUA using the transverse transmission technique (figure 1-4) [40].

In this study, the Sahara® system is used to provide simultaneous measurement of the SOS and BUA along with an empirical parameter called quantitative ultrasound index (QUI). The QUI, also known as stiffness index (SI), is an empirical index derived through a combination of the

BUA and SOS, which has been considered to be directly correlated to heel bone BMD values obtained by DXA [41]. The equation used to derive the QUI is specific to each QUS machine and for the Sahara® system is given as [41]:

QUI = 0.41(SOS+BUA) – 571 (1-23)

1.4.1.3 QUS Attenuation Measurement

The frequency dependent attenuation is obtained using equation 1-20 without the thickness dependent *x* in dB:

$$\alpha_{dB} = 20\ log\left[\frac{p_o(0)}{p_o(x)}\right] \quad (1\text{-}24)$$

where $p_o(0)$ is the pressure of the reference signal (water) and $p_o(x)$ is the pressure through the sample and reference material. By determining the attenuation through a range of frequencies from 0.2 to 1 MHz, linear dependence of attenuation versus frequency can be obtained. The slope of attenuation versus frequency is the broadband ultrasound attenuation coefficient BUA (dB/MHz) [2].

1.4.1.4 QUS Speed of Sound Measurement

In order to calculate the speed of sound (*c*), two time of flight (TOF) measurements are required. First the signal is being transmitted through the reference material (water) where equation 1-27 is used, and the second signal is being transmitted through both the reference material and the sample whose thickness is *t*, given by equation 1-28.

Reference material: $TOF^{ref} = \frac{L}{c^{ref}}$ (1-25)

The difference in these two signals is given by:

Reference material and sample: $TOF = \frac{L-t}{c^{ref}} + \frac{l}{c}$ (1-26)

Difference signal: $\Delta TOF = \frac{t}{c} - \frac{t}{c^{ref}}$ (1-27)

The speed of sound can then be expressed as [7]:

$$c = \frac{1}{\left(\frac{1}{c^{ref}}\right)+\left(\frac{\Delta TOF}{t}\right)} \tag{1-28}$$

If measurements are taken using transducers with direct contact with the skin then the reference signal needs not be considered and the equation 28 will become:

$$c = \frac{l}{TOF} \tag{1-29}$$

1.5 BONE-MIMICKING TISSUE PHANTOMS

Previously, studies have been conducted toward developing trabecular bone-mimicking phantoms and testing their validity using QUS. Materials that have been used included acrylic, carbon fiber plastics, ebonite, epoxy, perplex block, cuboid and nylon wires, all of which were used to study the relationship between SOS and BUA and bone characteristics [40–46]. Phantoms mimicking trabecular bone made by Tatarinov et al. [46] used different materials that include ebonite, acrylic plastic, fiberglass, carbon fiber plastic. Such materials possess varying stiffness, hence representing varying bone mineralization. They also made phantoms by mixing epoxy resin with “small quasi-cylindrical rubber” particles. Each phantom consisted of different volumes of particles so that the effect of porosity on ultrasound was observed [42]. Hodgskinson et al. [49] also built a phantom to study the relationship between porosity and BUA. They developed a cancellous phantom by using a Perspex block. They created two blocks: one with no holes and the other with holes. Additionally, the holes were increased in size (diameter) to characterize different porosities [44]. A study using polyacetal cuboid phantoms were used to represent cancellous bone. This cuboid had tiny holes to simulate the porosity of bone. Since these holes have fixed spacing, the porosity is changed by changing the position where the tissue mimicking phantom is placed [45]. Nylon-based phantoms have been developed to mimic similar properties to trabecular bone

[44, 45]. Epoxy resin phantoms were created by Tatarinov et al. [48] and Clarke [50], where one used gelatin-water based and the other rubber granules to simulate varying porosities. Besides these materials, hydroxyapatite has also been used in a previous study using epoxy and varying concentrations of calcium hydroxyapatite mimicking cortical bone, where the bone reference plates cover the hydroxyapatite concentration range for "osteoporotic bone (BMD < 1.2 g/cm^3) up to a relatively high BMD of 1.96 g/cm^3 for healthy bone" [3].

1.6 THESIS HYPOTHESIS AND SPECIFIC AIMS

Currently DXA is used as a gold-standard diagnostic modality for osteoporosis. However, DXA cannot be used on patients with strontium present in bone due to its attenuating properties of x-rays. An alternative method is needed, to be able to properly diagnose osteoporosis for patients with presence of strontium in their bones. The purpose of this study is to use the quantitative ultrasound (QUS) based modality to demonstrate independency of its performance to the presence of strontium in bone. To accomplish this, the goals of this study are as follows:

- To develop a new bone-mimicking phantom that is ultrasonically equivalent to bone.
- To dope the developed bone-mimicking phantom with various strontium concentrations.
- To make use of the QUS modality, as an alternative to DXA, to investigate whether the presence of strontium at various concentrations in human bone can have an impact on the ultrasound output.

1.7 REFERENCES FOR CHAPTER 1

[1] C. Njeh, D. Hans, T. Fuerst, C.-C. Glucer, and H. Genant, Eds., *Quantitative ultrasound: assessment of osteoporosis and bone status*. London, UK: Martin Dunitz, 1999.

[2] R. S. C. Cobbold, *Foundations of biomedical ultrasound*. Oxford ; New York: Oxford University Press, 2007.

[3] P. Laugier and G. Haïat, *Bone quantitative ultrasound*. Dordrecht; New York: Springer Science+Business media B.V., 2011.

[4] J. A. Kanis, "Diagnosis of osteoporosis and assessment of fracture risk," *The Lancet*, vol. 359, no. 9321, pp. 1929–1936, Jun. 2002.

[5] R. Bartl, *Osteoporosis: diagnosis, prevention, therapy*, 2nd ed. New York: Springer, 2009.

[6] S. L. Bonnick, *Bone densitometry in clinical practice: application and interpretation*, 3rd ed. New York, NY: Humana, 2010.

[7] W. Kalender, K. Engelke, T. P. Fuerst, C.-C. Gl¨uer, P. Laugier, and J. Shepherd, "Quantitative Aspects of Bone Densitometry," *J. ICRU*, vol. 9, no. 1, pp. 1–115, Apr. 2009.

[8] "Assessment of fracture risk and its application to screening for postmenopausal osteoporosis. Report of a WHO Study Group," *World Health Organ. Tech. Rep. Ser.*, vol. 843, pp. 1–129, 1994.

[9] B. L. Riggs and A. M. Parfitt, "Drugs Used to Treat Osteoporosis: The Critical Need for a Uniform Nomenclature Based on Their Action on Bone Remodeling," *J. Bone Miner. Res.*, vol. 20, no. 2, pp. 177–184, Nov. 2004.

[10] W. E. Cabrera, I. Schrooten, M. E. De Broe, and P. C. D'Haese, "Strontium and Bone," *J. Bone Miner. Res.*, vol. 14, no. 5, pp. 661–668, 1999.

[11] S. Pors Nielsen, “The biological role of strontium,” *Bone*, vol. 35, no. 3, pp. 583–588, Sep. 2004.

[12] P. J. Meunier, C. Roux, S. Ortolani, M. Diaz-Curiel, J. Compston, P. Marquis, C. Cormier, G. Isaia, J. Badurski, J. D. Wark, J. Collette, and J. Y. Reginster, “Effects of long-term strontium ranelate treatment on vertebral fracture risk in postmenopausal women with osteoporosis,” *Osteoporos. Int.*, vol. 20, no. 10, pp. 1663–1673, Oct. 2009.

[13] G. Boivin and P. J. Meunier, “The mineralization of bone tissue: a forgotten dimension in osteoporosis research,” *Osteoporos. Int. J. Establ. Result Coop. Eur. Found. Osteoporos. Natl. Osteoporos. Found. USA*, vol. 14 Suppl 3, pp. S19–24, 2003.

[14] S. . Dahl, P. Allain, P. . Marie, Y. Mauras, G. Boivin, P. Ammann, Y. Tsouderos, P. . Delmas, and C. Christiansen, “Incorporation and distribution of strontium in bone,” *Bone*, vol. 28, no. 4, pp. 446–453, Apr. 2001.

[15] M. N. Khan and A. A. Khan, “Cancer treatment-related bone loss: a review and synthesis of the literature,” *Curr. Oncol. Tor. Ont*, vol. 15, no. Suppl 1, pp. S30–40, Jan. 2008.

[16] P. Delannoy, D. Bazot, and P. J. Marie, “Long-term treatment with strontium ranelate increases vertebral bone mass without deleterious effect in mice,” *Metabolism*, vol. 51, no. 7, pp. 906–911, Jul. 2002.

[17] J. Buehler, P. Chappuis, J. L. Saffar, Y. Tsouderos, and A. Vignery, “Strontium ranelate inhibits bone resorption while maintaining bone formation in alveolar bone in monkeys (Macaca fascicularis),” *Bone*, vol. 29, no. 2, pp. 176–179, Aug. 2001.

[18] B. Habermann, K. Kafchitsas, G. Olender, P. Augat, and A. Kurth, “Strontium ranelate enhances callus strength more than PTH 1-34 in an osteoporotic rat model of fracture healing,” *Calcif. Tissue Int.*, vol. 86, no. 1, pp. 82–89, Jan. 2010.

[19] Y. F. Li, E. Luo, G. Feng, S. S. Zhu, J. H. Li, and J. Hu, "Systemic treatment with strontium ranelate promotes tibial fracture healing in ovariectomized rats," *Osteoporos. Int. J. Establ. Result Coop. Eur. Found. Osteoporos. Natl. Osteoporos. Found. USA*, vol. 21, no. 11, pp. 1889–1897, Nov. 2010.

[20] P. J. Marie, M. Hott, D. Modrowski, C. De Pollak, J. Guillemain, P. Deloffre, and Y. Tsouderos, "An uncoupling agent containing strontium prevents bone loss by depressing bone resorption and maintaining bone formation in estrogen-deficient rats," *J. Bone Miner. Res. Off. J. Am. Soc. Bone Miner. Res.*, vol. 8, no. 5, pp. 607–615, May 1993.

[21] J. Y. Reginster, R. Deroisy, M. Dougados, I. Jupsin, J. Colette, and C. Roux, "Prevention of early postmenopausal bone loss by strontium ranelate: the randomized, two-year, double-masked, dose-ranging, placebo-controlled PREVOS trial," *Osteoporos. Int. J. Establ. Result Coop. Eur. Found. Osteoporos. Natl. Osteoporos. Found. USA*, vol. 13, no. 12, pp. 925–931, Dec. 2002.

[22] J.-Y. Reginster, M. Hiligsmann, and O. Bruyere, "Strontium ranelate: long-term efficacy against vertebral, nonvertebral and hip fractures in patients with postmenopausal osteoporosis," *Ther. Adv. Musculoskelet. Dis.*, vol. 2, no. 3, pp. 133–143, Jun. 2010.

[23] W. E. Cabrera, I. Schrooten, M. E. De Broe, and P. C. D'Haese, "Strontium and Bone," *J. Bone Miner. Res.*, vol. 14, no. 5, pp. 661–668, May 1999.

[24] L. Oste, A. R. Bervoets, G. J. Behets, G. Dams, R. L. Marijnissen, H. Geryl, L. V. Lamberts, S. C. Verberckmoes, V. O. Van Hoof, M. E. De Broe, and P. C. D'Haese, "Time-evolution and reversibility of strontium-induced osteomalacia in chronic renal failure rats," *Kidney Int.*, vol. 67, no. 3, pp. 920–930, Mar. 2005.

[25] E. Seeman, “Pathogenesis of bone fragility in women and men,” *Lancet Lond. Engl.*, vol. 359, no. 9320, pp. 1841–1850, May 2002.

[26] S. P. Nielsen, D. Slosman, O. H. Sørensen, B. Basse-Cathalinat, P. De Cassin, C. Roux, and P. J. Meunier, “Influence of Strontium on Bone Mineral Density and Bone Mineral Content Measurements by Dual X-Ray Absorptiometry,” *J. Clin. Densitom*, vol. 2, no. 4, pp. 371–379, 1999.

[27] C. A. Mautalen and B. Oliveri, “Densitometric Manifestations in Age-Related Bone Loss,” in *The Aging Skeleton*, Elsevier, 1999, pp. 263–276.

[28] A. Pietrobelli, Z. Wang, C. Formica, and S. B. Heymsfield, “Dual-energy X-ray absorptiometry: fat estimation errors due to variation in soft tissue hydration,” *Am. J. Physiol.*, vol. 274, no. 5 Pt 1, pp. E808–816, May 1998.

[29] E. B. Podgoršak, *Radiation physics for medical physicists*, 2nd, enl. ed. Heidelberg: Springer, 2010.

[30] J. L. Prince and J. M. Links, *Medical imaging signals and systems*. Upper Saddle River, NJ: Pearson Prentice Hall, 2006.

[31] S. L. Bonnick and L. A. Lewis, *Bone densitometry for technologists*, 2nd ed. Totowa, N.J: Humana Press, 2006.

[32] J. Lilley, B. G. Walters, D. A. Heath, and Z. Drolc, “In vivo and in vitro precision for bone density measured by dual-energy X-ray absorption,” *Osteoporos. Int. J. Establ. Result Coop. Eur. Found. Osteoporos. Natl. Osteoporos. Found. USA*, vol. 1, no. 3, pp. 141–146, Jun. 1991.

[33] J. E. Adams, “Osteoporosis and bone mineral densitometry,” *Curr. Opin. Radiol*, vol. 4, no. 6, pp. 11–20, 1992.

[34] E. M. Alhava, “Bone density measurements,” *Calcif. Tissue Int.*, vol. 49 Suppl, pp. S21–23, 1991.

[35] C. C. Glüer, G. Blake, Y. Lu, B. A. Blunt, M. Jergas, and H. K. Genant, “Accurate assessment of precision errors: how to measure the reproducibility of bone densitometry techniques,” *Osteoporos. Int. J. Establ. Result Coop. Eur. Found. Osteoporos. Natl. Osteoporos. Found. USA*, vol. 5, no. 4, pp. 262–270, 1995.

[36] M. A. Laskey, A. J. Crisp, T. J. Cole, and J. E. Compston, “Comparison of the effect of different reference data on Lunar DPX and Hologic QDR-1000 dual-energy X-ray absorptiometers,” *Br. J. Radiol.*, vol. 65, no. 780, pp. 1124–1129, Dec. 1992.

[37] C. Wüster, F. de Terlizzi, S. Becker, M. Cadossi, R. Cadossi, and R. Müller, “Usefulness of quantitative ultrasound in evaluating structural and mechanical properties of bone: comparison of ultrasound, dual-energy X-ray absorptiometry, micro-computed tomography, and mechanical testing of human phalanges in vitro,” *Technol. Health Care Off. J. Eur. Soc. Eng. Med.*, vol. 13, no. 6, pp. 497–510, 2005.

[38] P. R. Hoskins, K. Martin, and A. Thrush, Eds., *Diagnostic ultrasound: physics and equipment*, 2nd ed. Cambridge, UK ; New York: Cambridge University Press, 2010.

[39] G. Haïat, F. Padilla, R. Barkmann, S. Kolta, C. Latremouille, C.-C. Glüer, and P. Laugier, “In vitro speed of sound measurement at intact human femur specimens,” *Ultrasound Med. Biol.*, vol. 31, no. 7, pp. 987–996, Jul. 2005.

[40] C. M. Langton, S. B. Palmer, and R. W. Porter, “The Measurement of Broadband Ultrasonic Attenuation in Cancellous Bone,” *Eng. Med.*, vol. 13, no. 2, pp. 89–91, Apr. 1984.

[41] S. R. Pye, V. Devakumar, S. Boonen, H. Borghs, D. Vanderschueren, J. E. Adams, K. A. Ward, G. Bartfai, F. F. Casanueva, J. D. Finn, G. Forti, A. Giwercman, T. S. Han, I. T.

Huhtaniemi, K. Kula, M. E. J. Lean, N. Pendleton, M. Punab, A. J. Silman, F. C. W. Wu, T. W. O'Neill, and EMAS Study Group, "Influence of Lifestyle Factors on Quantitative Heel Ultrasound Measurements in Middle-Aged and Elderly Men," *Calcif. Tissue Int.*, vol. 86, no. 3, pp. 211–219, Mar. 2010.

[42] A. Tatarinov, N. Sarvazyan, and A. Sarvazyan, "Use of multiple acoustic wave modes for assessment of long bones: Model study," *Ultrasonics*, vol. 43, no. 8, pp. 672–680, Aug. 2005.

[43] J. Töyräs, H. Kröger, and J. S. Jurvelin, "Bone properties as estimated by mineral density, ultrasound attenuation, and velocity," *Bone*, vol. 25, no. 6, pp. 725–731, Dec. 1999.

[44] K. I. Lee and M. J. Choi, "Phase velocity and normalized broadband ultrasonic attenuation in Polyacetal cuboid bone-mimicking phantoms," *J. Acoust. Soc. Am.*, vol. 121, no. 6, p. EL263, 2007.

[45] J. Chen, "Measurement of guided mode wavenumbers in soft tissue–bone mimicking phantoms using ultrasonic axial transmission," *Phys. Med. Biol.*, vol. 57, no. 10, pp. 3025–3037, May 2012.

[46] K. A. Wear, "The dependencies of phase velocity and dispersion on volume fraction in cancellous-bone-mimicking phantoms," *J. Acoust. Soc. Am.*, vol. 125, no. 2, pp. 1197–1201, Feb. 2009.

[47] A. J. Clarke, J. A. Evans, J. G. Truscott, R. Milner, and M. A. Smith, "A phantom for quantitative ultrasound of trabecular bone," *Phys. Med. Biol.*, vol. 39, no. 10, pp. 1677–1687, Oct. 1994.

[48] A. Tatarinov, I. Pontaga, and U. Vilks, "Modeling the influence of mineral content and porosity on ultrasound parameters in bone by using synthetic phantoms," *Mech. Compos. Mater*, vol. 35, no. 2, pp. 147–154, Mar. 1999.

[49] R. Hodgskinson, C. F. Njeh, M. A. Whitehead, and C. M. Langton, "The non-linear relationship between BUA and porosity in cancellous bone," *Phys. Med. Biol.*, vol. 41, no. 11, pp. 2411–2420, Nov. 1996.

[50] J. B. Bulman, K. S. Ganezer, P. W. Halcrow, and I. Neeson, "Noncontact ultrasound imaging applied to cortical bone phantoms," *Med. Phys.*, vol. 39, no. 6, p. 3124, 2012.

CHAPTER 2: BONE MINERAL DENSITY MEASUREMENTS OF STRONTIUM-RICH TRABECULAR BONE MIMICKING PHANTOMS USING QUANTITATIVE ULTRASOUND

This chapter is a manuscript that was submitted to Medical Physics, an official science journal of the American Association of Physicists in Medicine (AAPM) and the Canadian Organization of Medical Physicists (COMP)/Canadian College of Physicists in Medicine (CCPM)/International Organization for Medical Physics (IOMP).

Manuscript#: 15-1895

Submission date: Dec. 9, 2015

Contribution of authors:

Bisma Rizvi conducted the literature review and the background information write up. She conducted all experiments and data collection outlined in this work. She contributed in developing the trabecular bone-mimicking phantoms by the concept behind the airtight container and the procedure of developing the trabecular bone-mimicking phantoms. Moreover, she performed the statistical analysis in this research and the discussion drawn from the results obtained.

The bone-mimicking phantoms are based on the pure hydroxyapatite bone phantoms developed by Eric Da Silva, who also provided assistance in preparing the novel bare bone and the multi-layer bone-mimicking phantoms for ultrasound based experiments completed in this study. Furthermore, he considerably contributed in the statistical analysis of data, review and formatting of the multiple versions of this manuscript.

Luba Slatkovska assisted in providing information on the clinical QUS system and helped in conducting experiments using this system. She also reviewed the manuscript and provided extensive feedback with her expertise in the field.

Angela Cheung contributed in designing the clinical QUS experiments and choosing of a proper statistical analysis method to apply to collected data. She also reviewed the manuscript and provided her feedback toward making the final version of the document.

The concept of using QUS and design and development of the research QUS system used in this study were originated by Jahan Tavakkoli. He also contributed in designing and developing of the concept of multi-layer bone-mimicking phantom. He contributed in designing of the overall experimental study and in the preparation and finalizing the manuscript.

Ana Pejović-Milić designed, provided funding and assembled the research team for this research study. Furthermore, the first draft of this manuscript was completed with her assistance. Her constant involvement and guidance throughout this research project and writing of the manuscript help completing it to perfection.

Bone mineral density measurements of strontium-rich trabecular bone - mimicking phantoms using quantitative ultrasound

Bisma Rizvi, Eric Da Silva, Jahan Tavakkoli, and Ana Pejović-Milić [1]

Ryerson University, Department of Physics, Toronto, Ontario, Canada

Luba Slatkovska and Angela M. Cheung

University Health Network, Osteoporosis Program,

Toronto, Ontario, Canada; and University of Toronto,

Centre of Excellence in Skeletal Health Assessment, Toronto, Ontario, Canada

(Dated: December 9, 2015)

This study investigates the dependence of bone mineral density (BMD) determinations, obtained using quantitative ultrasound (QUS), on bone strontium content using a new generations of trabecular bone-mimicking phantoms. A new generation of bone-mimicking phantoms, consisting of hydroxyapatite (HA) and gelatin, were developed. In the phantom design, castor oil was added to create a multi-layer bone-mimicking phantom. These phantoms were measured using two QUS: the clinical Sahara® system and a research system with two matched pairs of transducers with center frequency of 1MHz. Similar to the clinical system, the research ultrasound system showed a strong dependency between BMD and broadband ultrasound attenuation (BUA), indicating a potential for QUS to be used as a means of estimating BMD ($p = 0.001$). There was no correlation between BMD and speed of sound (SOS) ($p = 0.546$). There was no correlation observed between BUA and increasing bone strontium levels for the research ($p = 0.749$) and clinical ($p = 0.609$) QUS systems. Similarly, no

[1] anamilic@ryerson.ca

dependency was observed and clinical ($p = 0.609$) QUS systems. Similarly, no dependency was observed between the SOS and bone strontium levels up to 3mol/mol [Sr/(Sr+Ca)]% for the research ($p = 0.862$) and clinical ($p = 0.481$) QUS systems. No effect on quantitative ultrasound index (QUI) values was observed with changing strontium levels with either research ($p = 0.939$) or clinical QUS systems ($p = 0.931$). A Bland-Altman analysis showed that there was a clear offset in determined QUI values for both systems but they are in agreement with one another.

2.1 INTRODUCTION

Osteoporosis is a bone deteriorating disease that can cause low-trauma fractures, pain and loss of independence to those afflicted. Osteoporosis is characterized by low bone mass and microarchitectural deterioration of bone tissue, which lead to enhanced bone fragility and increased fracture risk [1]. Low-trauma hip and spinal fractures, which are some of the most common and serious osteoporotic fractures, can also lead to an increased risk of morbidity and mortality in the osteoporotic population [2, 3].

Dual energy X-ray absorptiometry (DXA) is currently the clinical gold standard for the diagnosis and treatment monitoring of osteoporosis [4]. It is used to determine areal bone mineral density (*a*BMD), to help establish patients' risk for bone fractures [5]. It is a non-invasive diagnostic tool that measures *a*BMD (primarily of the hip and lumbar spine bones) based on the attenuation of X-rays through the patient. In this technique, two different X-ray energies are used as a means of providing a correction for X-ray attenuation by the overlaying soft tissue, thus providing an estimate of the bone's *a*BMD.

Strontium renalate, a strontium salt of ranelic acid, is a proposed drug for osteoporosis treatment that inhibits bone resorption and promotes bone formation [6]. Since strontium ($Z = 38$) has a higher atomic number than calcium ($Z = 20$), this leads to a greater attenuation of X-rays. Hence, strontium in bone leads to an overestimation of *a*BMD values obtained by DXA [7, 8]. Nielsen et al. [8], who studied this phenomenon using strontium-substituted apatite phantoms, made of calcium and strontium hydroxyapatite (HA), reported the apparent degree of *a*BMD overestimation of approximately 10% of *a*BMD for every 1mol/mol% Sr/(Ca + Sr).

Quantitative ultrasound (QUS) is another diagnostic modality for the estimation of BMD, which is used in research and clinical practice as an adjunct or alternative modality to DXA [5, 9]. It is an ultrasound-based modality, which measures the broadband ultrasound attenuation (BUA) and speed of sound (SOS) parameters to predict BMD. The method is thus non-invasive, does not require the use of ionizing radiation and is comparatively more portable and less expensive than DXA. Contrary to DXA measurements, QUS-based BMD assessments have been performed mostly at the calcaneus using an ultrasound transmit-through technique, which is a clinically approved modality backed by a large body of scientific and clinical studies [9–12]. These studies reported the existence of a direct relationship between BMD and both BUA and SOS [13–19], therefore proposing the use of QUS as an alternative diagnostic tool to DXA for BMD measurements. A review of various clinical calcaneal QUS devices can be found elsewhere [20, 21].

To examine the clinical utility of the calcaneal QUS system, Dane et al. [22] and Trimpou et al.[23] both conducted studies on postmenopausal women that portrayed a moderate association of both BUA and SOS on the *a*BMD of the lumbar spine and femur, as assessed by DXA. In the case of premenopausal women, SOS was seen to be significantly correlated to *a*BMD at the lumbar

spine and femur [22]. Further, other studies documented the ability of QUS to predict osteoporotic fracture in men [24, 25].

Human bone consists of two compartments: cortical and trabecular. The majority of clinical QUS studies have been performed on the calcaneal bone [9], which is composed of 95% trabecular bone [26]. Laugier et al. [27] determined the BUA and SOS in an *in vitro* study on trabecular cubes, obtained from the calcaneal human bone, with the BUA values ranging from 5.8 to 18.2dB/(cm·MHz) and the SOS ranging from 1485 to 1550m/s [27]. Trabecular bone-mimicking phantoms are desired for QUS measurements [28].

Various bone-mimicking trabecular phantoms have been proposed for QUS composed of different materials, such as acrylic, carbon fiber plastics, ebonite, epoxy, perplex block and cuboid and nylon wires, all of which exhibit the dependence of SOS and BUA on BMD [29–34]. Despite the successful use of these various materials as phantom materials, hydroxyapatite (HA), a mineral of the apatite group that is the main inorganic constituent of bone, was only used in one study [35]. Bulman et al. [35] used epoxy and varying concentrations of commercially available bone reference plate with varying concentrations of calcium HA to mimic cortical bone.

The objective of this study was to determine if strontium concentrations present in bone, due to strontium-based treatments of bone, have an impact on QUS-based BMD measurements. This was accomplished by developing and testing a new generation of HA-based, ultrasonically equivalent calcaneal bone-mimicking phantom a suitable for QUS BMD measurements.

2.2 MATERIALS AND METHODS

2.2.1 Preparation of Trabecular Bone-Mimicking Phantom

To prepare bare bone trabecular-mimicking phantoms with varying BMD values, HA samples were made in-house using the method developed by Da Silva et al. [36, 37]. The HA phantoms were prepared with a constant (Ca+Sr)/P mole ratio of 1.67. Strontium-substituted phantoms were prepared by mixing dry reagents $CaHPO_4 \cdot 2H_2O$ (USP grade, Amresco, Solon, OH, USA) with $Ca(OH)_2$ (USP grade, Amresco, Solon, OH, USA) and $Sr(OH)_2 \cdot 8H_2O$ (99% 80 metals basis, Alfa Aesar, Ward Hill, MA, USA). A tungsten carbide ball mill (Mixer Mill MM 301, Retsch GmbH & Co., Haan, Germany) was used to grind $Sr(OH)_2 \cdot 8H_2O$ into a fine powder. All powders were weighted using an analytical balance to the nearest 0.01mg (GR-202, A & D Company Ltd., Tokyo, Japan).

A setting solution was added to the powdered mixture in a ratio of powder-to- liquid of 2:1 and allowed to set as outlined by Da Silva et al. [36]. The setting solution was 1M of Na_2HPO_4 (ACS grade, Amresco, Solon, OH, USA) 85 in 18.2MΩ·cm water drawn from a MilliQ R system (used throughout this work).

The dry HA samples were crushed using a tungsten carbide ball mill and each powdered HA sample was added to a 5%*w/w* porcine skin gelatin solution (Sigma Aldrich, Oakville, ON) to mimic different BMD levels of calcaneal bone , namely 50, 100, 150, 200, 250 and 300mg/cm^3 [38]. Gelatin was added to the HA to represent the bone marrow within the trabecular bone framework, as previously proposed by Clarke et al. [30]. A 5%*w/w* concentration of gelatin was selected because the higher gelatin concentrations produced additional air bubbles within the phantom, which cause the ultrasound beam to be highly attenuated negatively influencing the BUA and SOS determinations. This mixture was molded in an airtight container with dimensions of (6.5

× 2.5 × 6.5) cm^3. The 2.5cm width of bare-bone phantoms was chosen to represent the average thickness of the calcaneal bone in humans [39]. The length and the height of the phantom were chosen to accommodate the beam diameter of the ultrasound transducer within the phantom dimensions and to perform measurements at different locations to test for phantom homogeneity. A rotator was used for the duration of 3 hours to make homogeneous bone-mimicking phantoms to prevent the HA particles from settling and aggregating during the setting period of the gelatin. Following this step, the phantoms were placed in a refrigerator at 4˚C for 12 hours to solidify. To test for homogeneity of the prepared bone-mimicking phantoms, three measurements were conducted at three, randomly selected sites of each phantom.

The second set of trabecular bone-mimicking phantoms, with a constant BMD, was made to investigate the effect of strontium concentrations on the SOS and BUA measurements. The constant BMD of 200mg/cm^3 represents a healthy human calcaneal bone density [38]. This set of phantoms contained different concentrations of strontium ranging from 0 to 3mol/mol [Sr/(Sr+Ca)]% [8]. These phantoms were made using the same method and the same container (size and shape) as mentioned above.

The total mass density of the trabecular bone-mimicking phantoms was measured using Archimedes' Principle, while their BMD was calculated based on the amount of calcium HA added to the volume of each phantom.

2.2.2 Multi-Layer Trabecular Bone-Mimicking Phantoms

To mimic the overlying soft tissue layers present around the calcaneal bone, the trabecular-mimicking phantom was submerged in an acrylic container filled with castor oil (Clearwater Soap Works, BC, Canada), creating a multi-layer bone-mimicking phantom. Castor oil is a widely used liquid to mimic the ultrasound properties of soft tissue (BUA = 0.94dB/cm at 1MHz, SOS =

1540m/s) [40, 41]. The acrylic container was built to include two Mylar windows on each side of the container to provide the QUS transducers coupling required for the clinical QUS measurement. A 0.75cm layer of castor oil was chosen on each side of the bone phantom as representative of the overlying soft tissue surrounding the calcaneal bone as reported in the literature [42]. All bone-mimicking phantoms were placed inside the acrylic container filled with castor oil to make the multi-layer trabecular bone-mimicking phantoms, which ultrasonically simulated human trabecular bone with its overlying soft tissue and skin.

Both sets of phantoms, with varying BMD and strontium concentrations, were measured using two QUS systems: an in-house research system and a clinical QUS systems (Sahara®).

2.2.3 Research Quantitative Ultrasound System

To investigate the proof of principle of QUS, an ultrasound transmit-through system was designed and developed in our laboratory utilizing two separate single-element focused ultrasound transducers [43]. Two focused transducers (one as a transmitter and another as a receiver) were aligned along the same axis in a confocal configuration to obtain the maximum signal output. The parameters of each transducer were: aperture diameter = 3.17cm, focal length =10.1cm, and resonance frequency = 1MHz. These transducers were submerged in water and placed in an aligned confocal sample was positioned at the common foci of the transducers and the received signal transmitted through the 2.5cm thickness of the phantom was acquired using a digital oscilloscope (Model 7032A; Agilent Technologies, Santa Clara, CA, USA). To measure the SOS and the BUA of the multi-layer bone-mimicking phantom, a function generator (Model AFG3010; Tektronix, Beaverton, OR, USA) was used to transmit signal (transmitter) generating 30-cycle bursts of a single frequency ultrasound beam. The transmitted ultrasound signal was varied between 0.5 to 1.3MHz with 0.1MHz increments for these measurements.

The frequency spectrum of the measured signal was obtained, first by acquiring the signal from a reference medium (degassed and ionized water) without the multi-layer bone-mimicking phantom, and then by a second reading taken with the phantom in place. The linear regression of ultrasound attenuation versus frequency was used to determine the slope of the BUA with units of dB/MHz.

To account for the additional losses in received signal due to reflection at the boundaries, the acoustic impedance for both media Z_1 and Z_2 need to be known and considered in the reflection equation (Eqn. 1) as:

$$\frac{P_r}{P} = \frac{Z_1 - Z_2}{Z_1 + Z_2} \tag{1}$$

where Z_1 and Z_2 are acoustic impedances of water and the bone mimicking phantom, respectively.

To compensate for the reflection losses associated with both surfaces, the following correction factor (*CF*) (Eqn. 2) was then applied to all BUA measurements:

$$CF = \left(\frac{Z_1 - Z_2}{Z_1 + Z_2}\right)^2 \tag{2}$$

For the multi-layer trabecular bone-mimicking phantoms the impedance of castor oil is very close to water and thus the reflection loss due to castor oil can be neglected. The SOS values were measured using the standard 'time of flight' method [44], where the difference in the time of an ultrasound pulse traveling between the two transducers, with and without the phantom, was recorded. These transmit-through ultrasound measurements were performed on trabecular bone-mimicking and multi-layer trabecular bone-mimicking phantoms containing varying BMD and strontium concentrations. To verify the accuracy of the measurement, the research QUS system was tested using PVCP (Polyvinyl Chloride Plastisol, MF manufacturing Co., Fort Worth, Texas, USA) of known attenuation. Two ultrasound parameters, namely BUA and SOS, were measured and all measurements were performed in triplicate.

2.2.4 Clinical Quantitative Ultrasound System

Following the measurements on the research QUS system, the multi-layer bone-mimicking phantoms were measured using a clinical QUS system (Sahara®, Hologic Inc., Walthman, MA, USA). These measurements were performed by placing the acrylic container between the two-ultrasound probes of the system (a transmitter and a receiver), with transmit frequency range of 200-600 kHz. The system contained transducer pads, which require the application of Vaseline (Unilever, London, England) to make suitable contact with the phantom surface to permit the ultrasound beam to transmit through the phantom and be detected by the receiver. The calibration of the clinical system was performed on the day of each measurement, both before and after the measurement, using the manufacturer provided calibration phantom. The Sahara R system provides the simultaneous measurement of the SOS and BUA along with the quantitative ultrasound index (QUI). The QUI is an empirical index derived through a combination of the BUA and SOS, which has been shown to be directly correlated to the human calcaneal BMD values obtained by DXA [45]. The equation used to derive the QUI is specific to each QUS machine and correlates strongly with BMD (g/cm^2) at the heel. The QUI for the Sahara® system is given by Eqn. 3 [45]:

$$QUI = 0.41(SOS + BUA) - 571 \tag{3}$$

Only multi-layer phantoms were measured by the clinical QUS system. All phantoms used in this study were measured in triplicate on the clinical QUS system, with repositioning after the first and second measurement.

2.2.5 Statistical Treatment of Data

Statistical Package for the Social Sciences (SPSS) software version 22.0 (IBM, Armonk, NY, USA) was utilized to conduct statistical analyses of the obtained data. Linear regression in

the SPSS was used to determine the impact of changing BMD and strontium levels on BUA and SOS. A Bland-Altman analysis was performed to assess the association of QUI values determined by both systems.

2.3 RESULTS

2.3.1 Density of the Trabecular Bone-mimicking Phantoms

The BMD values of the new trabecular bone-mimicking phantoms were measured against their total mass density (Figure 1). The measured change in the total mass density of the trabecular bone-mimicking phantoms ranged from 1.03g/cm^3 to 1.27g/cm^3 when the BMD values were varied between 50mg/cm^3 and 300mg/cm^3. These BMD values were calculated by using the mass of hydroxyapatite (bone mineral) present within the volume of the phantom. In Figure 1 a linear trend is observed due to an increase in mass with constant volume.

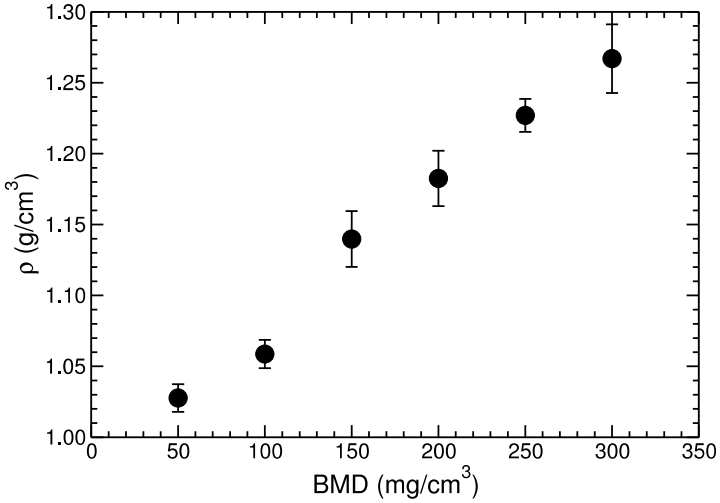

FIG. 1: The relationship between the measured phantom mass density (ρ) and calculated BMD of the trabecular bone-mimicking phantoms prepared for this study.

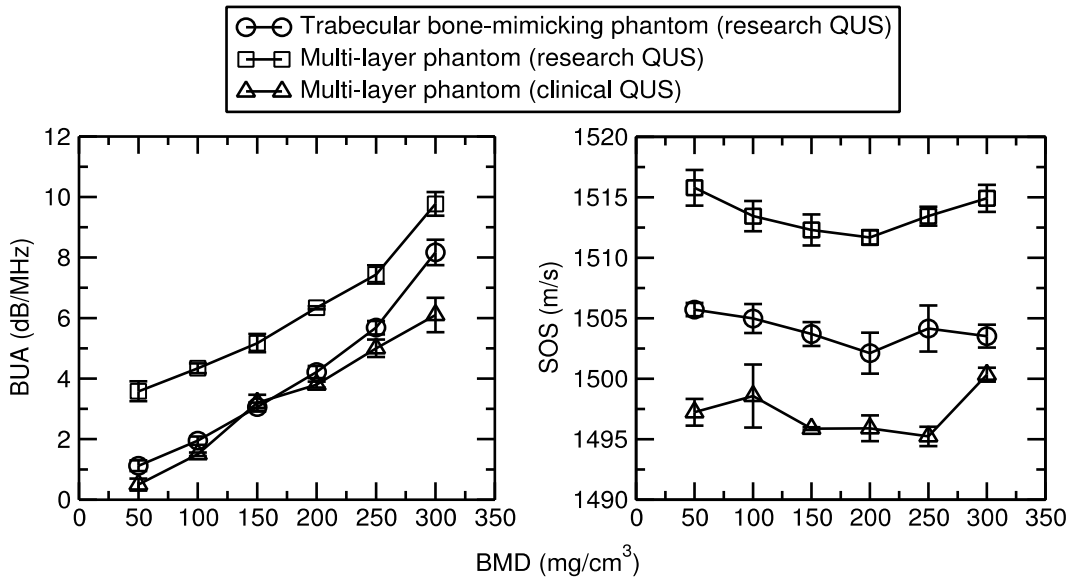

FIG. 2: Relationship between BUA and BMD, and, SOS and BMD, without any strontium present in trabecular bone-mimicking and multi-layer phantoms, as measured with the research and clinical QUS systems.

2.3.2 Quantitative Ultrasound Measurement of the Multi-Layer Trabecular Bone-Mimicking Phantoms

For the trabecular bone-mimicking phantoms, the research QUS system showed a strong association between the BUA and BMD ($p < 0.001$) (Figure 2). The observed association between the SOS and BMD was not statistically significant ($p = 0.163$) (Figure 2). The research QUS system also showed the same relationship for the multi-layer trabecular bone-mimicking phantoms, with BUA ($p = 0.001$) and SOS ($p = 0.546$). The clinical QUS system (using the multi-layer trabecular bone-mimicking phantoms) also demonstrated a strong dependence between BUA and BMD ($p = 0.001$), but no statistically significant dependence for SOS ($p = 0.238$).

The second set of multi-layer trabecular bone-mimicking phantoms, with a constant BMD concentration of 200mg/cm^3 and varying strontium concentrations, were measured using both the research and clinical QUS systems (Figure 3). The increase in the phantom's strontium concentration showed no significant effect on BUA (p = 0.749) or SOS (p = 0.862) measurements when the research QUS system was used. Similarly, using the clinical QUS system, the change in the strontium content did not statistically affect the BUA (p = 0.609) or SOS (p = 0.481) measurements.

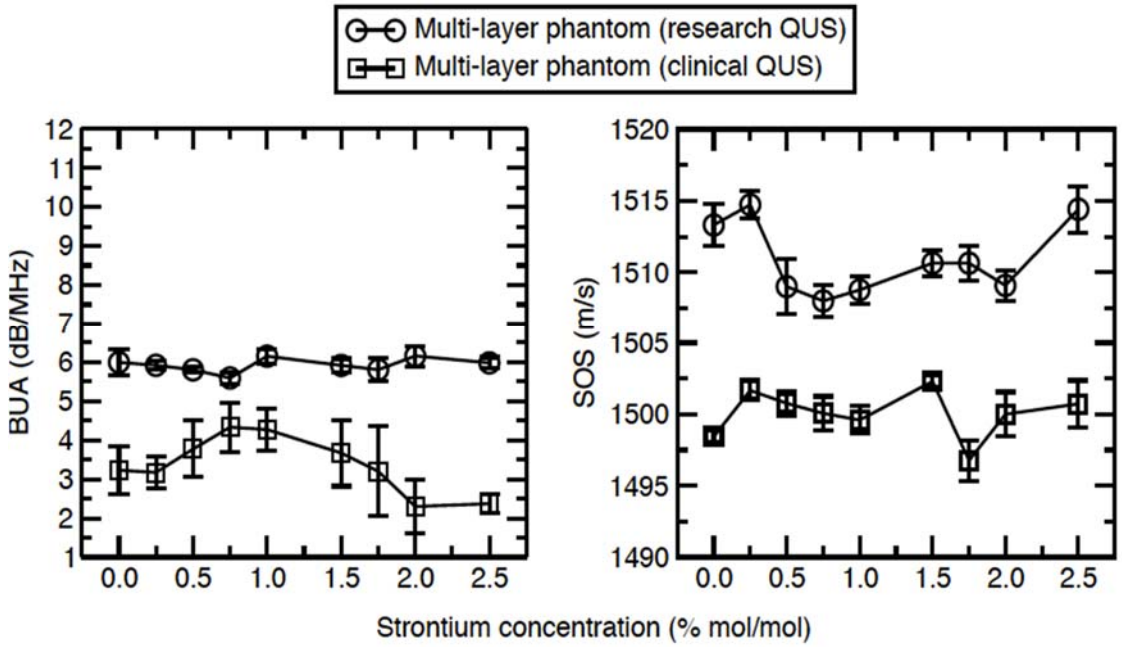

FIG. 3: The BUA and SOS as a function of strontium concentration, at a BMD of 200mg/cm^3.

2.3.3 Quantitative Ultrasound Index (QUI) of the Multi-Layer Trabecular Bone-Mimicking Phantoms

Figure 4 presents the QUI, defined by Eqn. 3, estimated at different strontium concentrations in the multi-layer trabecular bone mimicking phantoms, using the research and clinical QUS systems. No effect was observed on the QUI values with the changing level of strontium, neither with the research ($p = 0.939$) nor with the clinical ($p = 0.931$) QUS systems.

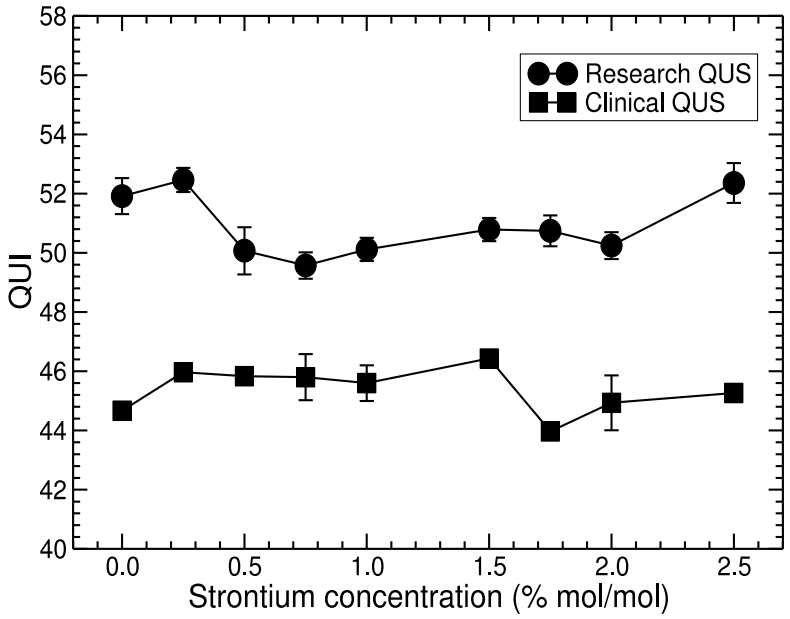

FIG. 4: The QUI as a function of strontium concentration in the multi-layer trabecular bone mimicking phantoms using the research and clinical QUS systems.

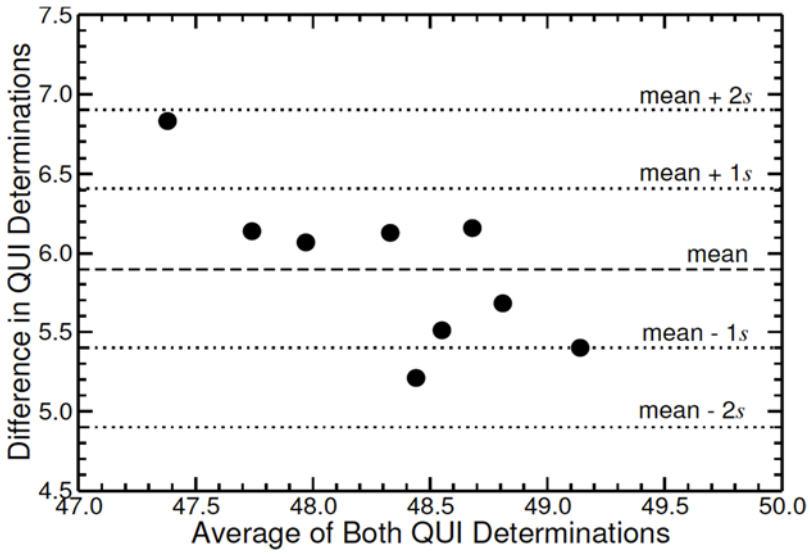

FIG. 5: Bland-Altman plot of the QUI determinations. Mean difference of 5.9 and standard deviation (*s*) of 0.5.

Bland-Altman analysis showed no systematic bias between the two QUS systems (Figure 4). There are offsets in measurements for BUA, SOS and QUI between the two systems (as shown in Figures 3 and 5).

2.4 DISCUSSION

Osteoporosis is a bone disease characterized by a low BMD and deterioration of bone microarchitecture. It is commonly diagnosed by evaluating the subject's BMD as measured by DXA. Two large randomized human studies reported the ability of strontium ranelate pharmacotherapy to reduce the incidence of fracture in females affected by postmenopausal osteoporosis: SOTI [46] and TROPOS [47]. The knowledge of the strontium concentration in the treated subjects became important once it was observed that bone strontium concentration influences the value of the BMD measurements by DXA [7, 8], and makes it difficult to establish that the strontium-based treatment benefits bones in terms of the increased BMD [48]. From the radiation physics point of view, owing to the higher atomic number of strontium versus calcium,

X-rays are more attenuated in the presence of strontium in bone. Thus an overestimation of BMD in a strontium-rich bone is expected and reported to be directly proportional to the strontium concentration [8].

An alternative diagnostic tool for the measurement of bone density is QUS. To the best of our knowledge, its use for the assessment of bone health of the strontium-rich human bone has not been reported in the scientific literature. The initial step in this work was the synthesis of strontium-free calcium HA phantoms [36, 37]. All HA based bone phantoms were prepared with a constant (Ca+Sr)/P mole ratio of 1.67. Following this step, calcium HA was substituted with strontium HA under a controlled condition, with a molar ratio range of 3mol/mol [Sr/(Sr+Ca)] [30] and mixed with gel, to simulate the densities of trabecular strontium-rich bone and the marrow within the trabecular framework.

A strong dependence between BUA and BMD (Figure 2) was observed which is in agreement with the observations of earlier studies [27, 49]. The measured BUA and SOS values (Figure 2), by both the research and the clinical QUS systems of the trabecular bone-mimicking and multi-layer trabecular bone-mimicking phantoms were within the experimental results reported on human trabecular bone of the calcaneal site, as 7.62 to 22.75dB/MHz for BUA, and 1485 to 1550m/s for SOS [27]. Therefore, the newly developed trabecular bone-mimicking phantoms were determined to be acceptable phantoms that mimic trabecular bone properties.

The ultrasound parameters measured versus changing strontium concentrations in the phantoms are depicted in (Figure 3). The measured BUA and SOS obtained using the clinical QUS system are similar to the experimental results reported by [50] for the human calcaneal bone. They reported the BUA and SOS ranges of 0.4 to 3.94dB/MHz and from 1412 to 1746m/s, respectively.

The SOS was previously reported to be directly proportional to BMD level [27], when the experiment was conducted using trabecular bone from the calcaneal site. In another study by Bulman et al. [35], cortical bone was simulated using epoxy with the added densities of HA ranging from 0 to 1.7mg/cm^3. The total mass density of these phantoms ranged from 1.15 to 2.25g/cm^3. An increase in SOS as a function of increased total mass density was observed, while at the lower total mass densities SOS remained constant. This slowly increasing linear trend is present due to an increase in compressibility and density. This characteristic of SOS being largely influenced by trabecular separation on trabecular cubes was reported before [49] and attributed to the fact that SOS may be more dependent on the trabecular separation. There might not have been sufficient scattering present in our trabecular bone-mimicking phantoms to cause a change in SOS. In our work, the lower BMDs were associated with a small change in the total mass density between the phantoms (1.03-1.27g/cm^3 in Figure 1), which may explain the observed independence of SOS from the low BMD associated with the trabecular bone phantoms. The reported SOS values (Figure 2) using the research QUS system on bone-mimicking phantoms were in the range of 1502 to 1506m/s with the standard error ranging from 0.68 to 1.90m/s and with the maximum percent difference from the average (1504 ± 2) of 0.12. This variation of SOS was insignificant with the varying trabecular BMD.

Nevertheless, the BUA values measured with the two QUS systems in our study are significantly different (Figure3). A similar discrepancy was also observed by Strelitzki et al. [51] using a bench-top system and two different clinical QUS systems, and it was attributed to the use of different systems with different operating parameters for the measurement of BUA. Other reasons may include the difference in transducer sizes and geometries (focused versus planar ones), and the amount of separation between them. Further, studies using dry and water based

systems [51, 52] concluded that BUA and SOS values were highly device dependent. Compare to wet systems, there is less control on the parameters such as temperature stability [31]. Also, the Sahara® QUS system pads are shaped to mirror the contour of the heel, whereas our multi-layer box contained flat parallel surfaces [52].

Furthermore, there is a disagreement between BUA values for the trabecular bone-mimicking phantoms comparing to the calcaneal *in vitro* observed in studies for the research and clinical system. This could be due to the fact that the phantoms do not have a concave surface nor have the internal spongy structure compared to the calcaneal bone. These differences can cause a change in reflection and refraction of ultrasound beams, accounting for differences in BUA values obtained from the two systems [52].

On the other hand, the SOS measurements of strontium rich bone-mimicking phantoms, with constant BMD of 200mg/cm^3 (Figure 3), were found to be statistically different between the research and clinical systems, and, therefore, seem to be dependent of the QUS systems. This outcome could be due to the fact that the measurements of SOS in the two systems are not similar. Since the clinical QUS system measured the bone phantom thickness in order to determine the SOS, this outcome was expected and it is supported by previously published work [52]. The QUI is an empirically-derived parameter based on the combination of two ultrasound parameters of the bone, BUA and SOS, as stated in Eqn. 3, and it was calculated for both QUS systems used in this study. The value of QUI is more heavily influenced by SOS, and less by BUA. The contribution to the difference in the QUI values between the research and the clinical QUS systems is mainly from the difference in the SOS values. As seen in Figure 3, the SOS values are not similar between the two QUS systems used in this work. Hence, it is expected and observed (Figure 4) that the QUI values obtained by the two ultrasound systems are statistically different ($p < 0.001$). Therefore, it

could be concluded that regardless of differences in values of estimated QUI , the two systems still have the ability to provide an estimated BMD reading independent of the strontium content present in phantoms as seen in (Figure 3). There is good agreement between the two systems (Figure 5) however there are offsets present in measurements of BUA, SOS and QUI (Figure 3).

The findings presented in this work could be relevant for the monitoring of BMD in individuals treated with strontium-based pharmacotherapy. The use of commercially available clinical QUS systems, instead of the clinical gold standard method DXA, for the diagnosis and/or monitoring of BMD, for the health assessment of strontium-rich bone could be a viable alternative available to clinicians in the future. Nevertheless, more research is required to fully evaluate clinical QUS systems and their applicability for this use.

2.5 CONCLUSIONS

In this work, we reported on the development of new calcium HA based trabecular bone-mimicking phantoms suitable for the use in any QUS system by obtaining ultrasound parameters closely mimicking trabecular bone. In addition, the results of BUA portray a direct relationship with BMD of these phantoms. The new phantoms, in turn, allowed the investigation of applicability of QUS measurements for BMD determination in the presence of strontium. We also reported that the QUS empirically-derived parameter, QUI, appears to be independent of the strontium concentration present in the trabecular bone-mimicking phantoms. The results of this study point to the applicability of the clinical QUS systems for the diagnosis and monitoring of BMD in individuals treated with strontium ranelate or strontium supplements recommended for the treatment or prevention of osteoporosis, whereas the BMD of these individuals cannot reliably be measured with DXA.

2.6 ACKNOWLEDGMENTS

The authors would like to thank Arthur Worthington and Graham Pearson for their technical support, and Elizabeth Berndl and Pooya Sobhe Bidari for their help in conducting experiments (all from the Department of Physics, Ryerson University). Funding for this research project was provided by a Natural Sciences and Engineering Research Council of Canada (NSERC) grant awarded to Dr. Ana Pejović-Milić.

2.7 REFERENCES

[1] E. Legrand, D. Chappard, C. Pascaretti, M. Duquenne, S. Krebs, V. Rohmer, M. F. Basle, and M. Audran, J. Bone Miner. Res. **15**, 13 (2000).

[2] R. Bartl and B. Frisch, *Osteoporosis: diagnosis, prevention, therapy* (Springer, Berlin, 2009).

[3] A. Pietrobelli, Z. Wang, C. Formica, and S. B. Heymsfield, Am. J. Physiol. **274**, E808 (1998).

[4] M. L. Frost, G. M. Blake, and I. Fogelman, Osteoporos. Int. **11**, 321 (2000).

[5] D. Hans, C. Durosier, J. A. Kanis, H. Johansson, A.-M. Schott-Pethelaz, and M.-A. Krieg, J. Bone Miner. Res. **23**, 1045 (2008).

[6] P. J. Meunier, C. Roux, S. Ortolani, M. Diaz-Curiel, J. Compston, P. Marquis, C. Cormier, G. Isaia, J. Badurski, J. D. Wark, J. Collette, and J.-Y. Reginster, Osteoporos. Int. **20**, 1663 (2009).

[7] J. Christoffersen, M. R. Christoffersen, N. Kolthoff, and O. Ba¨renholdt, Bone **20**, 47 (1997).

[8] S. P. Nielsen, D. Slosman, O. H. Sørensen, B. Basse-Cathalinat, C. P. De, C. Roux, and M. P. J, J. Clin. Densitom. **2**, 371 (1999).

[9] C. M. Langton and C. F. Njeh, IEEE Trans. Ultrason. Ferroelectr. Freq. Control **55**, 1546 (2008).

[10] R. Hodgskinson, C. F. Njeh, M. A. Whitehead, and C. M. Langton, Phys. Med. Biol **41**, 2411 (1996).

[11] C. M. Langton, C. F. Njeh, R. Hodgskinson, and J. D. Currey, Bone **18**, 495 (1996).

[12] M. L. McKelvie and S. B. Palmer, Phys. Med. Biol. **36**, 79 (1991).

[13] B. Cortet, N. Boutry, P. Dubois, I. Legroux-G´erot, A. Cotten, and X. Marchandise, Calcif. Tissue Int. **74**, 60 (2003). [14] D. Hans, A. M. Schott, and P. J. Meunier, Eur. J. Med. **2**,

157 (1993).

[15] D. Hans, T. Fuerst, and F. Duboeuf, Eur. Radiol. **7**, Suppl 2: S43 (1997).

[16] J. J. Kaufman and T. A. Einhorn, J. Bone Miner. Res. **8**, 517 (1993).

[17] C. F. Njeh, C. M. Boivin, and C. M. Langton, Osteoporos. Int **7**, 7 (1997).

[18] F. Padilla, F. Jenson, V. Bousson, F. Peyrin, and P. Laugier, Bone **42**, 1193 (2008).

[19] J. To¨yra¨s, H. Kro¨ger, and J. S. Jurvelin, Bone **25**, 725 (1999).

[20] C. Njeh, D. Hans, T. Fuerst, C. C. Glucer, and H. Genant, *Quantitative ultrasound: assessment of osteoporosis and bone status* (Martin Dunitz, London, UK, 1999).

[21] C. F. Njeh, T. Fuerst, E. Diessel, and H. K. Genant, Osteoporosis Int. **12**, 1 (2001).

[22] C. Dane, B. Dane, A. Cetin, and M. Erginbas, Climacteric **11**, 296 (2008).

[23] P. Trimpou, I. Bosaeus, B.-˚A. Bengtsson, and K. Landin-Wilhelmsen, Eur. J. Radiol. **73**, 360 (2010).

[24] S. Gonnelli, C. Cepollaro, L. Gennari, A. Montagnani, C. Caffarelli, D. Merlotti, S. Rossi, A. Cadirni, and R. Nuti, 315 Osteoporos. Int. **16**, 963 (2005).

[25] S. M´esza´ros, E. To´th, V. Ferencz, E. Csupor, E. Hosszu´, and C. Horva´th, Joint Bone Spine´ **74**, 79 (2007).

[26] E. Jagelaviciene, A. Krasauskiene, R. Zalinkevicius, R. Kubilius, and I. Vaitkeviciene, Dentomaxillofacial Radiol. **42**, 20120050 (2013).

[27] P. Laugier, P. Droin, A. M. Laval-Jeantet, and G. Berger, Bone **20**, 157 (1997).

[28] M. A. Krieg, R. Barkmann, S. Gonnelli, A. Stewart, D. C. Bauer, L. D. R. Barquero, J. J. Kaufman, R. Lorenc, P. D. Miller, W. P. Olszynski, C. Poiana, A. M. Schott, E. M. Lewiecki, and D. Hans, J. Clin. Densitom. **11**, 163 (2008).

[29] J. Chen, Phys. Med. Biol. **57**, 3025 (2012).

[30] A. J. Clarke, J. A. Evans, J. G. Truscott, R. Milner, and M. A. Smith, Phys. Med. Biol. **39**, 1677 (1994).

[31] P. Laugier and G. Ha¨ıat, *Bone quantitative ultrasound* (Springer, New York, 2011).

[32] K. I. Lee and M. J. Choi, J. Acoust. Soc. Am. **121**, EL263 (2007).

[33] A. Tatarinov, I. Pontaga, and U. Vilks, Mech. Compos. Mater. **35**, 147 (1999).

[34] K. A. Wear, J. Acoust. Soc. Am. **125**, 1197 (2009).

[35] J. B. Bulman, K. S. Ganezer, P. W. Halcrow, and I. Neeson, Med. Phys. **39**, 3124 (2012).

[36] E. Da Silva, B. Kirkham, D. V. Heyd, and A. Pejović-Milić, Anal. Chem. **85**, 9189 (2013).

[37] E. Da Silva, D. V. Heyd, B. Rizvi, and A. Pejović-Milić, Biomed. Phys. Eng. Express, Submitted (2015).

[38] C. Kang and R. Speller, Br. J. Radiol. **71**, 861 (1998).

[39] P.-J. Chen, T. Chen, M.-C. Lu, and W.-J. Yao, Meas. Sci. Technol. **16**, 1349 (2005).

[40] R. C. Preston, *Output Measurements for Medical Ultrasound* (Springer, London, 1991).

[41] F. A. Duck, *Physical Properties of Tissue* (Academic Press, London, 1990).

[42] C. Chappard, E. Camus, F. Lefebvre, G. Guillot, J. Bittoun, G. Berger, and P. Laugier, J. Clin. Densitom. **3**, 121.

[43] S. Rahimian and J. Tavakkoli, J. Ther. Ultrasound **1**, 14 (2013).

[44] W. Kalender, K. Engelke, T. P. Fuerst, C.-C. G. er, P. Laugier, and J. Shepherd, J. ICRU **9**, 1 (2009).

[45] S. R. Pye, V. Devakumar, S. Boonen, H. Borghs, D. Vanderschueren, J. E. Adams, K. A. Ward, G. Bartfai, F. F. Casanueva, J. D. Finn, G. Forti, A. Giwercman, T. S. Han, I. T. Huhtaniemi, K. Kula, M. E. Lean, N. Pendleton, M. Punab, A. J. 340 Silman, F. C. Wu, T. W. O'Neill, and E. S. Group, Calcif. Tissue Int. **86**, 211 (2010).

[46] P. J. Meunier, C. Roux, E. Seeman, S. Ortolani, J. E. Badurski, T. D. Spector, J. Cannata, A. Balogh, E.-M. Lemmel, S. Pors-Nielsen, R. Rizzoli, H. K. Genant, and J.-Y. Reginster, N. Engl. J. Med. **350**, 459 (2004).

[47] J. Y. Reginster, E. Seeman, V. De, C. A. S. M, J. Compston, C. Phenekos, J. P. Devogelaer, M. D. Curiel, A. Sawicki, S. Goemaere, O. H. Sorensen, D. Felsenberg, and P. J. Meunier, J. Clin. Endocrinol. Metab. **90**, 2816 (2005). 345 [48] G. M. Blake and I. Fogelman, J. Clin. Densitom. **10**, 34 (2007).

[49] C. C. Gluer, C. Y. Wu, M. Jergas, S. A. Goldstein, and H. K. Genant, Calcif. Tissue Int. **55**, 46 (1994).

[50] N. R. Portero-Muzy, P. M. Chavassieux, D. Mitton, F. Duboeuf, P. D. Delmas, and P. J. Meunier, Calcif. Tissue Int. **81**, 92 (2007).

[51] R. Strelitzki, Osteoporos. Int. **6**, 471 (1996).

[52] R. Strelitzki and J. G. Truscott, Osteoporos. Int. **8**, 104 (1998).

CHAPTER 3:DISCUSSIONS, CONCLUSIONS, AND FUTURE WORK

3.1 DISCUSSIONS

Osteoporosis is a serious concern and is widely recognized as an important public health problem because of morbidity, mortality and cost due to fractures [1]. It occurs due to change in the rate of the metabolism of bone, which causes a decrease in the overall BMD. DXA is the current gold standard method used to determine the changes in BMD using T-score and Z-scores. It is based on the fundamental principle of a through transmission technique which utilizes X-rays at two different energies. BMD measurements can be influenced by an element with a higher atomic number than calcium such as strontium [2]. Strontium is an element that has therapeutic properties shown in several studies, however, due to its position in the periodic table, it can attenuates x-rays more than calcium. This can lead to an incorrect reading in the BMD measurements and therefore DXA cannot be used for monitoring or diagnosing osteoporosis for patients who are on strontium-based medications [3]. Quantitative ultrasound (QUS) could potentially be an alternative method to properly diagnose osteoporosis for patients with presence of strontium in bone. Two QUS systems, a research system and a clinical device were used in this study on strontium-rich bone-mimicking phantoms. To this end, new bone-mimicking phantoms with varying BMD levels and different strontium concentrations were developed. Two QUS physical parameters and one derived clinical parameter were investigated in this study: broadband ultrasound attenuation (BUA), speed of sound (SOS), and quantitative ultrasound index (QUI). Based on the results obtained in this study, a linear correlation is observed between the BMD values and the QUI values obtained with both QUS systems ($p<0.001$ for the research and $p=0.001$

for the clinical systems). However, no statistical correlation was observed between the two systems for the SOS values measured (p=0.163 for the research and p=0.546 for the clinical systems). Also, the values measured for BUA and SOS were within the reported values for human trabecular bone. These results provide evidence that the QUS technique is able to differentiate the BMD values in bone-mimicking phantoms with a similar trend as observed by DXA. Following this initial step, bone-mimicking phantoms of constant BMD of 200 mg/cm^3 were doped with 0 to 3 mol/mol% [Sr/Sr+Ca] to evaluate the effect of strontium concentration on the QUS measurements. There was no statistical correlation observed with the BUA (p=0.749) nor the SOS (p=0.862) for research system. Similar results were obtained for the clinical QUS system (BUA (p=0.609) and SOS (p=0.481). An additional parameter was derived for the clinical QUS system called QUI. There was no effect observed in the QUI values with increasing concentrations of strontium for the research (p=0.939) and clinical (p=0.931) QUS systems. Bland-Altman statistical analysis [3] was performed between the QUI values obtained with the two systems and resulted in a good agreement between the two systems, however there was an offset between the values.

3.2 CONCLUSIONS

In conclusion, the development of new trabecular bone-mimicking phantoms doped with strontium allowed for the determination of the effect of strontium on the BMD measurements using the QUS systems. It is demonstrated in this study that the two different QUS systems are both capable of providing the actual BMD measurements independent of the bone strontium content. The outcome of this study could potentially be relevant for monitoring of bone mineral density in osteoporotic patients who are being treated with strontium-based drugs or self-supplemented using strontium-based supplements.

3.3 FUTURE WORK

The results from this study portrayed that the presence of strontium in trabecular bone-mimicking phantoms has no effect on the clinical and the research QUS system parameters. This was accomplished by the development of bone-mimicking phantoms containing different concentrations of strontium.

The multi-layer trabecular bone-mimicking phantoms can further be developed by utilizing different materials that mimic bone and soft tissue: such as acrylic, carbon fibber plastics, ebonite, epoxy, perplex block, cuboid and nylon wires). Although the advantage of using 5% gelatine is that it exhibits negligible ultrasound attenuation and hence the majority of the attenuation is due the added material/compounds within the phantoms, alternative materials could be used to better mimic the bone porosity and change of its composition due to the changes in bone health associated with different stages of osteoporosis.

In this experiment strontium was introduced into the phantoms to study its impact on QUS parameters. However, other elements accumulated in bone besides strontium (such as lead, aluminum, zinc, etc.) can be added to these phantoms to investigate their effect on the BMD measured with clinical modalities. Additionally, these phantoms can also be used in experiments with different modalities other than DXA and QUS such as QCT (quantitative computed tomography).

Several improvements can be implemented in the current design of the bone-mimicking phantom such as: incorporating a more efficient acoustic window in the phantom box, and using a more efficient coupling medium, such as standard ultrasound gel, to couple the phantom to the clinical QUS transducers.

The next step of this project should be the measurement of the same set of new bone mimicking phantoms on the clinical DXA and QUS modalities to validate the usefulness of QUS for the BMD measurement of strontium rich bone. Finally, this study should eventually be extended to *in vivo* animal and clinical human studies to investigate the effect of excess amount of various relevant chemical elements such as strontium in bone and to compare the performances of two main osteoporosis diagnostic modalities, i.e. DXA and QUS, in these conditions.

3.4 REFERENCES FOR CHAPTER 3

[1] W. E. Cabrera, I. Schrooten, M. E. De Broe, and P. C. D'Haese, "Strontium and Bone," *J. Bone Miner. Res.*, vol. 14, no. 5, pp. 661–668, 1999.

[2] J. A. Kanis, "Diagnosis of osteoporosis and assessment of fracture risk," *The Lancet*, vol. 359, no. 9321, pp. 1929–1936, Jun. 2002.

[3] S. K. Hanneman, "Design, Analysis, and Interpretation of Method-Comparison Studies:," *AACN Adv. Crit. Care*, vol. 19, no. 2, pp. 223–234, Apr. 2008.

Appendix A: Procedure for Developing Trabecular Bone-mimicking Phantoms

Constructing bone-mimicking phantom:

1. Hydroxyapatite (HA) bone phantoms were made using the method given by Da Silva et al [1]. These phantoms contained different concentrations of strontium ranging from 0 to 3 mol/mol % expected in human bone as reported in the literature [2].
2. The bone-mimicking material was crushed in a ball mill using a frequency of 30 cycles/second and the resulting powder was added to a porcine skin gelatine (Sigma Aldrich, Oakville, ON) and water mixture solution to mimic different bone density of calcaneal bone, ranging from 50 to 250 mg/cm^3. This mixture was moulded in an airtight container with dimensions 6.5cm × 2.5cm × 6.5cm (see Figure A-1).
3. A rotator was used for duration of 3 hours to make homogeneous bone-mimicking phantoms to prevent the particles from settling.
4. The phantoms were placed in a fridge for 12 hours to get dried and solidified.

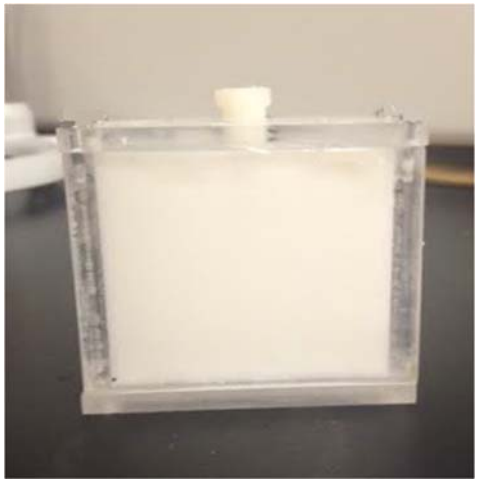

Figure A-1. Bone-mimicking phantom mould containing HA and gelatine.

Constructing an airtight container:

1. First step is to use a container with dimensions 6.5cm × 2.5cm × 6.5cm and to drill a hole on one side of the container to put the mixture inside the container once everything is sealed.
2. Place silicon sealant on top of the container to seal one side of the container.
3. Then place a saran wrap on top and cover it up with a lid and tape it down so the saran wrap stays in its place until the glue is dry.
4. Next, pour the mixture of HA and gelatine into the airtight container once the glue is dry.

Appendix B: Figures of Multi-layer Bone-mimicking Phantom and QUS Systems used in this Study

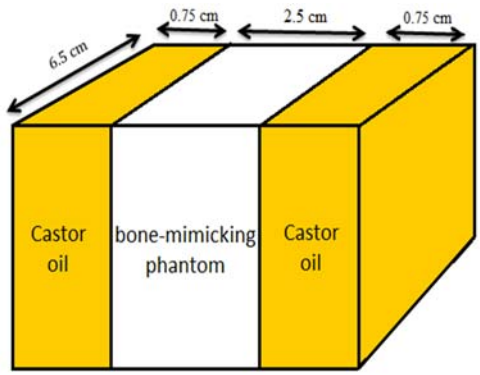

Figure B-1. Schematic design of the multi-layer bone-mimicking phantom using castor oil to mimic soft tissue.

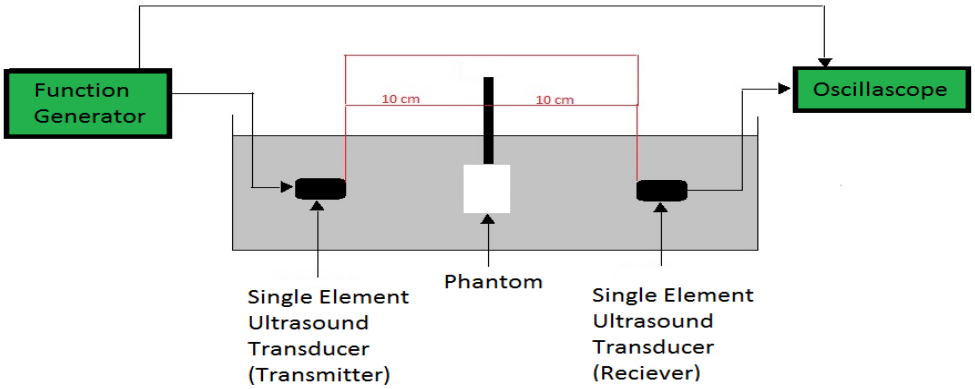

Figure B-2. Schematic experimental setup of research QUS system for determination of BUA and SOS.

Figure B-3: Schematic experimental setup of clinical QUS (Hologic Sahara® QUS system) with acrylic container for the determination of BUA and SOS.

Appendix C: Plot of QUI vs. BMD

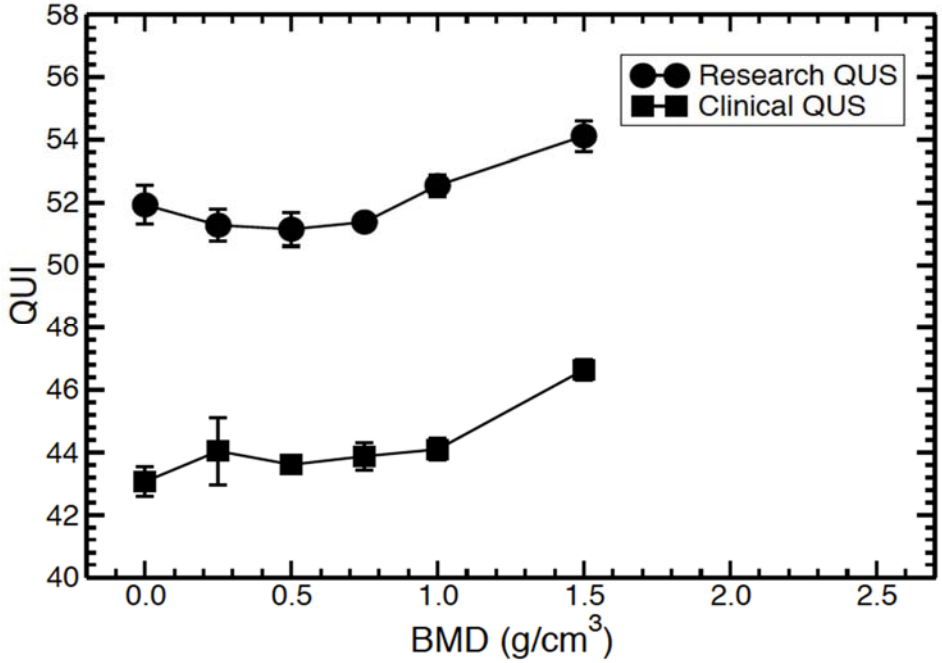

Figure C-1: The QUI as a function of BMD concentration in the multi-layer trabecular bone mimicking phantoms using the research and clinical QUS systems.

Appendix D: Measurements of BUA and SOS

The SOS was determined using:

$$c = \frac{1}{\left(\frac{1}{c^{ref}}\right)+\left(\frac{\Delta TOF}{t}\right)}$$

where c^{ref} is the speed of sound in water which is determined based on the temperature:

$$c^{ref} = 1405.03 + 4.624T - 3.83 \times 10^{-2}T^2$$

ΔTOF is the difference in time of arrivals two ultrasound signals.

t = the thickness of the phantom.

The BUA was determined using:

$$\alpha_{dB} = 20\ log\left[\frac{p_o(0)}{p_o(x)}\right]$$

where $p_o(0)$ is the amplitude pressure of the reference signal and $p_o(x)$ is the amplitude pressure of the signal received with both the phantom and the reference present.

References for Appendices

[1] E. Da Silva, B. Kirkham, D. V. Heyd, and A. Pejović-Milić, "Pure Hydroxyapatite Phantoms for the Calibration of in Vivo X-ray Fluorescence Systems of Bone Lead and Strontium Quantification," *Anal. Chem.*, vol. 85, no. 19, pp. 9189–9195, Oct. 2013.